Opto-Electronic Science

Review

2022, Vol. 1, No. 5

DOI: 10.29026/oes.2022.210007

Functional nonlinear optical nanoparticles synthesized by laser ablation

Lianwei Chen and Minghui Hong*

Nonlinear optics is an important research direction with various applications in laser manufacturing, fabrication of nanostructure, sensor design, optoelectronics, biophotonics, quantum optics, etc. Nonlinear optical materials are the fundamental building blocks, which are critical for broad fields ranging from scientific research, industrial production, to military. Nanoparticles demonstrate great potential due to their flexibility to be engineered and their enhanced nonlinear optical properties superior to their bulk counterparts. Synthesis of nanoparticles by laser ablation proves to be a green, efficient, and universal physical approach, versatile for fast one-step synthesis and potential mass production. In this review, the development and latest progress of nonlinear optical nanoparticles synthesized by laser ablation are summarized, which demonstrates its capability for enhanced performance and multiple functions. The theory of optical nonlinear absorption, experimental process of laser ablation, applications, and outlooks are covered. Potential for nanoparticle systems is yet to be fully discovered, which offers opportunities to make various types of next-generation functional devices.

Keywords: nonlinear optics; nanoparticles; optical limiting; saturable absorption; laser ablation

Chen LW, Hong MH. Functional nonlinear optical nanoparticles synthesized by laser ablation. *Opto-Electron Sci* **1**, 210007 (2022).

Introduction

Nonlinear optics is the study of nonlinear responses from the interaction of intense light with matter. Nanoparticles fabricated by laser ablation have been extensively used in nonlinear optics. A nonlinear optical effect typically describes a process in which the optical properties of a material change nonlinearly as a consequence of the strong irradiation of incident light[1]. For most nonlinear optical effects, an intensified incident light is required to trigger the nonlinear effects that can be observed. The study of nonlinear optics started when Franken and coworkers firstly observed the second-harmonic generation in 1961, right after the demonstration of a functional laser system by Maiman one year before. Since then, various nonlinear optical effects have been discovered and this field has grown continuously into an important branch of modern optics. After many years of development, nonlinear optics has become the pillars for many frontier research and widely used systems, including laser fabrication, optical imaging, information processing & communications, as well as nanoscale lithography[2–6]. Advances in this topic can potentially boost many disciplines. Nonlinear optical effects include optical Kerr effect which leads to an intensity-dependent refractive index, optical limiting, saturable absorption, nonlinear scattering, multiple-photon absorption, frequency-mixing process, second/third/high harmonic generation, optical parametric amplification, optical rectification, up/down conversion, etc. Nonlinear optical effects can be generally categorized into three groups, depending on the corresponding light properties: 1) nonlinear effect to modify the light wavelength, 2) nonlinear effect to change the light refraction, 3) nonlinear effect to vary the light amplitude/intensity. In this review, we

Department of Electrical and Computer Engineering, National University of Singapore, 4 Engineering Drive 3, 117576, Singapore.

*Correspondence: MH Hong, E-mail: elehmh@nus.edu.sg

Received: 10 September 2021; Accepted: 27 October 2021; Published online: 20 May 2022

shall primarily focus on the nonlinear optics of the third group related to the light amplitude and intensity.

In this group, saturable absorption and optical limiting are two nonlinear phenomena to describe the transmission change of a material system[7–9]. Saturable absorption is the process when the light absorption decreases with light intensity. In other words, a material with the saturable absorption tends to be more "transparent" under stronger incident light irradiation. Materials with the saturable absorption are widely used to fabricate high power lasers. For example, it can construct the cavity for Q-switching, which produces a pulsed output. It is also the candidate to build logic circuits for next-generation optical computers. On the other hand, optical limiting describes the opposite effect. An optical limiting material reduces the transmission of light when the light intensity increases. Hence, optical limiting is also denoted as the reverse saturable absorption. Optical limiting is also a critical effect with applications ranging from protective materials, military weapons, optical switching, to high power laser sources. In spite of their importance, both saturable absorption and optical limiting normally require incident light with high intensity. Hence, they are mostly observed in devices using a pulsed laser with high peak power. This condition can possibly result in permanent optical damage. It is also a critical bottleneck to limit practical applications for the complicated design and high cost of high power lasers. The investigation of suitable materials with superior nonlinear properties is a primary research direction in this field. The progress shall not only greatly promote the performance of current optical nonlinear systems, but also bring about new opportunities to design functional devices to address the increasing needs for quantum optics, advanced sensors, artificial intelligence, next-generation optical computers, and many other frontier topics[10–12].

Nanotechnologies have paved the ways to engineer new materials and break the conventional limits for nonlinear optics. Nanoparticles are one of the most important members that are widely studied, which has a long history of thousands of years. The initial utilization of nanoparticles for optical purposes dated back to the 5th century BC, when nanoparticles were prepared for decorative purposes and changed the color of the object in both China and Egypt[13]. In the past decade, optical devices and components based on nonlinear optical nanoparticles are receiving more and more attention due to their enhanced performance and multifunctional capabilities. The following primary advantages make them suitable for many applications compared to their bulk counterparts: 1) **Plasmonic properties:** metallic nanoparticles present active surface plasmonic resonance under light excitation, which demonstrates intense optical absorption or scattering across the regions from visible to near-infrared spectrum (NIR). The plasmonic properties of nanoparticles can be modified by engineering their composition, shape, and geometry, which offers great flexibility to fulfill requirements for different applications. With this feature, metallic nanoparticles are extensively used in nonlinear optical devices. 2) **Surface functionalization:** nanoparticles' decorated surfaces can be easily functionalized by a wide range of organic molecules, which makes nonlinear optical nanoparticles highly flexible for different matrixes or integrated with other technologies. 3) **Stability and compatibility:** many nanoparticles are chemically and physically stable. Specific nanoparticles, such as nano-diamonds, can stand extremely high temperatures and pressures. Many of them also show good biocompatibility, which extends the application scope for nonlinear optical devices.

Attributed to the above advantages, nanoparticles are widely used for nonlinear optical applications. For the nanoparticles' synthesis, how to produce nonlinear optical nanoparticles with large scale, high repeatability, and low cost remains to be a challenge. To address this challenge, various synthesis approaches have been investigated. Chemical and laser ablation approaches are two of the primary synthesis methods. Chemical approaches are useful to produce nanoparticles at an industrial scale. For chemical approaches, there also exist limitations including impurities and agglomeration. On the other hand, laser ablation is a more direct, environmentally friendly, and universal method for the synthesis of nonlinear optical nanoparticles[14–18]. Laser ablation is a dynamic process to remove target materials from a solid substrate under high power short pulse laser irradiation. It can be conducted in air, liquid, and vacuum; combined with external electrical or magnetic fields, chemical reactions, and pre/post treatment; it can achieve various purposes, including surface engineering, defect modification, and fragmentation[19–22]. Great flexibility and possibilities are offered for applications based on nonlinear optical nanoparticles to fulfill the requirements of different devices[23–33].

Recently, an increasing number of researches focus on optical devices with nonlinear optical nano-particles to

address the bottleneck challenges in this field. Systems based on nanoparticles are highly versatile and powerful compared to optical systems based on conventional bulk nonlinear optical materials. Systems based on nonlinear optical nanoparticles have two advantages: 1) they are multi-functional with the flexibility to meet the requirements for different applications; 2) they offer superior performance by further engineering nanoparticles and the hosting systems[26,31]. This review summarizes the recent progresses in this direction, which focuses more on the methodologies with a series of case studies as the illumination. It also covers extended topics to provide additional views on their key advantages and achievements. The challenges and future research trends are another focus, with the latest research works to introduce new opportunities and potential. This review is organized with the following structure. The first section "Basic theory and experimental setups for nanoparticles' synthesis" aims to provide a brief introduction to the fundamentals and background information. The theoretical part contains the basic knowledge of nonlinear optics and the experimental part covers the experimental setup design and parameters' optimization. The second section "Nonlinear optical nanoparticles' production, functions, and applications" firstly focuses on the nanoparticles as the central building blocks in nonlinear optical systems. Key features of nanoparticles and methods for their property modification are summarized. Applications and potentials are presented to provide the landscape for the current field of nonlinear optical nanoparticle systems. The final part of this review focuses on challenges and outlooks to highlight future opportunities in this research field.

Basic theory of nonlinear optics and experimental setups for nanoparticles' synthesis

Fundamentals for nonlinear optics

To understand the optical nonlinear effect, it is helpful to present the model to quantitatively describe the nonlinear effect. Material's response to the incidence of an external electromagnetic field in the linear case can be described by the following equation:

$$\boldsymbol{P} = \varepsilon_0 x^1 \boldsymbol{E}\,, \tag{1}$$

where $\boldsymbol{P}$ is the polarization of material system, ε_0 is the permittivity of free space, and x^1 indicates the linear susceptibility of material, and $\boldsymbol{E}$ represents the electric field introduced by the electromagnetic wave. The applied electromagnetic field interacts linearly with the materials as described by this equation. In the case of nonlinear optics, Eq. (1) can be further generalized by introducing the nonlinear terms of different orders:

$$\boldsymbol{P} = \varepsilon_0 x^1 \boldsymbol{E} + \varepsilon_0 x^2 \boldsymbol{E}^2 + \varepsilon_0 x^3 \boldsymbol{E}^3 + \cdots\,, \tag{2}$$

where x^2 and x^3 are the second- and third- order nonlinear optical susceptibilities of materials. The term $\varepsilon_0 x^2$ and $\varepsilon_0 x^3$ are also commonly defined as the second- and third-order nonlinear polarizabilities of materials caused by different physical mechanisms. Various types of nonlinear effects can be understood by substituting the above polarization and susceptibilities with the nonlinear terms of the material system into the Maxwell equations and deriving a set of nonlinear electromagnetic wave equations with higher-order terms. These equations provide the theoretical bases to describe how the material systems react. The further expansion and detail derivation for different nonlinear effects can be found in the classic book of nonlinear optics[34].

Based on the nonlinear electromagnetic equations, the nonlinear optical process also involves the interaction of multiple photons and excitation of the electrons of the materials systems, which can be used to understand the saturable absorption. A simplified schematic involving two photons is presented in Fig. 1. ω_1 and ω_2 denote photons. The solid line is the ground energy state for the electrons in the material system and dash lines stand for excited states[1]. In this process, the electron absorbs both photons and is excited to the energy state with higher energy. The possibility of the electron to enter the excited states 1 and 2 are denoted as $\boldsymbol{P}_1$ and $\boldsymbol{P}_2$ (such possibility is also denoted as the cross-section). After the excitation, those electrons can also release the energy and come back to the ground state. For the linear absorption, the incident light is weak. Most of the electrons are in the ground state. The absorption of the material is dominated by $\boldsymbol{P}_1$. However, in a nonlinear optical process, the incident light is intensified, electrons can be excited both from the group state to the first excited state and from the first excited state to the second excited state, which is indicated by the arrows in the figure. In this case, the absorption of the material depends both on $\boldsymbol{P}_1$ and $\boldsymbol{P}_2$. In the case of the saturable absorption, $\boldsymbol{P}_2$ is smaller than $\boldsymbol{P}_1$. In other words, those excited electrons are less likely to further absorb photons and jump to higher states. From the macro-scale perspective, the material

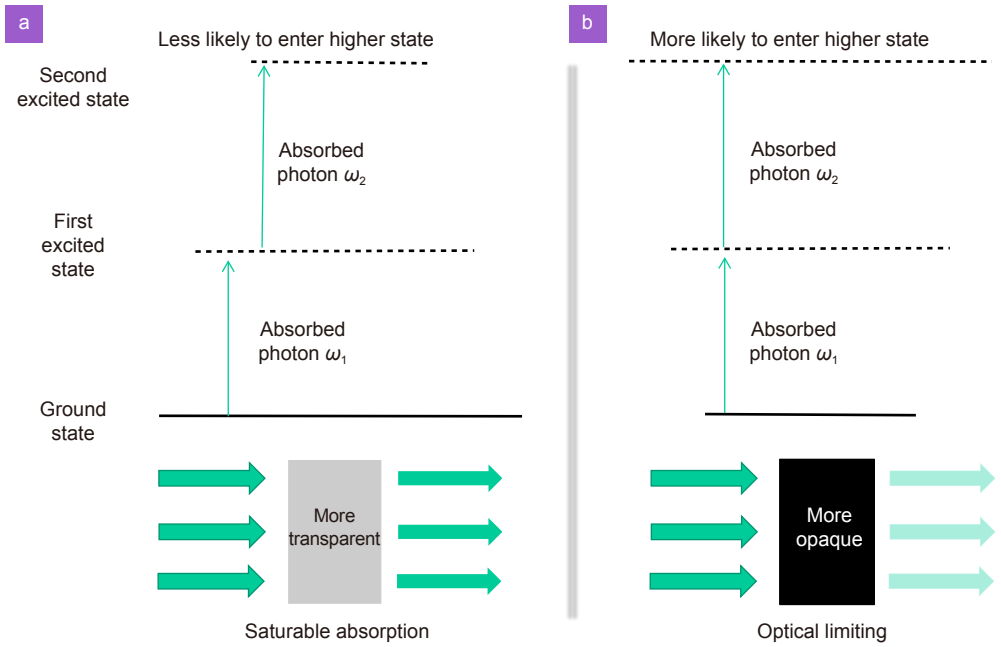

Fig. 1 | Schematics of nonlinear processes. (**a**) Saturable absorption. (**b**) Optical limiting[1].

"saturates" and absorbs fewer photons. For these materials, the transmittance increases for the incident light at a higher intensity. It also explains why the optical nonlinear process normally requires high power laser to maintain the electrons in high energy states. For the case of the reverse saturable absorption (optical limiting), $\boldsymbol{P}_2$ is larger than $\boldsymbol{P}_1$. The material absorbs more photons when the electrons are excited and the transmittance drops. $\boldsymbol{P}_1$ and $\boldsymbol{P}_2$ depend on many factors of the materials system as well as the environment. The practical case is more complicated than the simplified illumination above. Hence, it is more convenient to propose a model to link the nonlinear absorption coefficient directly with the intensity of incident light. The following equation is widely used to describe the nonlinear optical absorption:

$$\alpha(I) = \alpha_0 + \beta I\,, \tag{3}$$

where α is the nonlinear absorption coefficient at different intensities, α_0 is the linear absorption coefficient, I indicates the light intensity, and β is a parameter known as the nonlinear absorption coefficient depending on materials. Equation (3) directly describes the nonlinearity of the material by the nonlinear coefficients that can be measured experimentally, which is useful to quantitatively characterize the nonlinear performance of the system. As demonstrated in the following sections, the nonlinear absorption coefficient is one of the most important parameters to determine the functionality of nonlinear systems. Most researches in this field focus on how to fabricate materials with large nonlinear coefficients, improve conventional systems based on nonlinear materials, and design nonlinear devices to address new challenges. Many factors can be studied. For example, the morphology of the nanoparticles affects their optical responses, especially for the metallic nanoparticles, as the surface plasmon resonance is mostly determined by the material, shape, and size. For the metallic nanoparticles, if the shape is not isotropic, their optical responses depend on the polarization states of light. In addition, the asymmetric nanoparticles can also be used to control light polarization in the nanoscale, revealing great potentials for many nonlinear optical devices sensitive to the light polarization[35]. Similarly, the morphology of the nanoparticles also influences other optical properties including transmittance and absorption. These optical properties are important for nonlinear optical performance. For example, the transmittance is critical for both saturable absorption and optical limiting. The absorption is critical for the up-conversion and frequency mixing. Hence, the morphology engineering of the nanoparticles is one important research direction.

Z-scan technology

Besides the theoretical investigation, experimental approaches need to be designed to measure nonlinear coefficients for different material systems. Many methods have been designed. Among them, Z-scan technology is a widely used technique to effectively measure both nonlinear absorption and refractive index. Z-scan was

invented in 1989 and became well-known for its simplicity and high sensitivity[36]. The schematic of a Z-scan setup is shown in Fig. 2. It works on the principle of moving samples in the optical path of a focused Gaussian laser beam. To achieve it, the Gaussian beam is firstly focused by a lens and the focal spot is marked as the zero position. The direction of the optical path is denoted as the Z axis. Along the Z axis, the light intensity keeps increasing until it reaches the maximum at the focal spot (zero position). As the sample scans along the Z axis, it experiences different light intensities depending on its position. A detector is positioned at the end of the Z axis to record transmitted light power. To compare the detected light intensity with input light intensity, the sample's transmittance can be calculated. Hence, the transmittances at different laser intensities can be plotted in a single scan cycle and the information of its nonlinearities can be extracted by analyzing the plot. Depending on nonlinear coefficients to be characterized, two types of Z-scan techniques have been developed, namely the closed aperture and open aperture Z-scans. For the closed aperture Z-scan, an aperture is positioned before the detector as shown in Fig. 2(a). With the aperture, only a portion of the transmitted light can be captured by the detector. It makes the measurement sensitive to the change of laser beam, such as spreading or focusing. When the sample locates at different Z positions, its nonlinear refraction causes the change of the laser beam and the light intensity captured by the detector varies accordingly. Hence, its nonlinearity can be measured by scanning the sample along the Z axis and recording the transmittance.

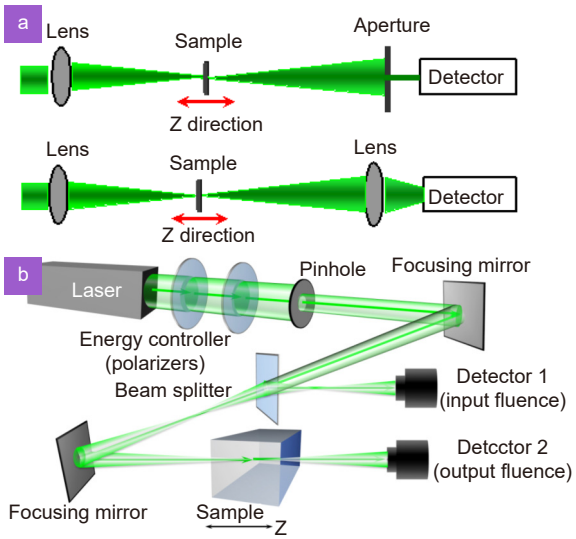

Fig. 2 | Experimental setups of Z-scan. (**a**) Open aperture and close aperture Z-scan systems. (**b**) Components to construct the open aperture Z-scan with tunable incident laser power[62].

However, the closed aperture Z-scan has one issue when measuring the nonlinear refraction. For most materials, nonlinear refraction and nonlinear absorption coexist. Hence, the transmittance measured by the detector is also affected by the nonlinear absorption of the material. To address this challenge, the open aperture Z-scan technique was invented. For the open aperture Z-scan setup, most of the components are the same as the closed aperture Z-scan, except that a focal lens is added before the detector as demonstrated in Fig. 2(a). While only a portion of the transmitted light can be captured by the detector for the closed aperture Z-scan, this additional focal lens is used to focus all the light into the detector. As the detector captures all the light, the nonlinear refraction no longer affects the measurement. Hence, the transmittance only depends on the nonlinear absorption. The transmittance at different Z positions can be used to calculate the nonlinear absorption coefficient. A typical open aperture Z-scan experimental setup is demonstrated in Fig. 2(b). The laser source provides light at the desired wavelength. The light intensity can be controlled by a pair of polarizers. A pinhole is added after the polarizers to control the waist of the laser beam. The beam splitter is used to split the laser beam and measure the input intensity as the reference. A lens is used to focus the laser beam and create the light profile desired for the Z-scan. The sample is put on a translational stage to move along the Z axis. A detector is used to capture all the light transmitted through the sample. In this setup, the sensing area of the detector is large enough so no focal lens is needed. Otherwise, an additional lens is required to ensure all the transmitted light is detected.

The data measured in a Z-scan cycle can be used to plot the measured transmittance at different Z positions. Fitting this curve with the formula derived by the theoretical models allows calculating the nonlinear coefficients. For the nonlinear absorption, the coefficients can be written as Eq. (3). The normalized transmittance at different Z positions can be derived as:[37]

$$T(z)=\frac{1}{\sqrt{\pi}q_0(z)}\int_{-\infty}^{\infty}\ln\left[1+q_0(z)\,\mathrm{e}^{-\tau^2}\right]\mathrm{d}\tau\,, \tag{4}$$

$$q_0(z)=\frac{\beta I_0 L_{\mathrm{eff}}}{1+\dfrac{z^2}{z_0^2}}\,, \tag{5}$$

$$L_{\text{eff}} = \frac{1 - \mathrm{e}^{-\alpha_0 L}}{\alpha_0}, \tag{6}$$

for $|q_0| < 0$, Eq. (4) can be written as:

$$T(z) = \sum\nolimits_{m=0}^{\infty} \frac{[-q_0(z)]^m}{(m+1)^{\frac{3}{2}}}, \tag{7}$$

where $z_0 = k\omega_0^2/2$ is known as Rayleigh length or diffraction length of the beam. $k = 2\pi/\lambda$ the wave vector. ω_0 the waist radius of the input laser beam at focus. L_{eff} the effective length of the sample, α_0 and β the linear and nonlinear absorption coefficients same as Eq. (3), λ the incident laser wavelength, I_0 the incident laser beam intensity, and L the sample thickness. Fitting $T(z)$ to different points on the Z-scan curve can calculate the nonlinear absorption coefficients of material.

Similarly, numerical fitting can also be used to calculate the nonlinear refraction coefficients from the data of the closed aperture Z-scan. The transmittance is affected by both the nonlinear absorption and nonlinear refraction. Hence, the optical nonlinear absorption at each point should firstly be calculated from the open aperture Z-scan. To achieve this purpose, the normalized transmittance for the closed aperture Z-scan is divided by transmittance of the open aperture Z-scan at the same experimental conditions. Then, the following equations derived from the theoretical model can be used for fitting: [37]

$$T(z) = \frac{\int_{-\infty}^{\infty} P_{\text{t}}(t)\left[\Delta\varphi_0(t)\right]\mathrm{d}t}{S\int_{-\infty}^{\infty} P_{\text{i}}(t)\,\mathrm{d}t}, \tag{8}$$

$$P_{\text{i}}(t) = \pi{\omega_0}^2 I_0(t)/2, \tag{9}$$

$$S = 1 - \exp\left(-\frac{2r_{\text{a}}^2}{\omega_{\text{a}}^2}\right), \tag{10}$$

$$\Delta\varphi_0 = k\Delta n(t) L_{\text{eff}}, \tag{11}$$

$$\Delta n = \gamma I_0(t), \tag{12}$$

where $P_{\text{t}}(t)$ is the transmitted power through the aperture, which can be obtained by spatially integrating the electric field at the aperture; $P_{\text{i}}(t)$ the instantaneous input laser power, S the linear transmittance through the aperture, $\Delta\varphi_0$ the phase shift introduced by the nonlinear refraction of the sample, Δn the variance of refractive index. ω_0, I_0, k, and L_{eff} are defined the same as the previous nonlinear absorption calculation, r_{a} the radius of the aperture, ω_{a} the beam radius at the aperture, γ the nonlinear refraction coefficient, which is the parameter of interests. By fitting Eq. (8) with the data collected in the closed aperture Z-scan measurement, one important feature of the nonlinear curve is identified:

$$\Delta T_{\text{p-v}} \cong 0.406(1-S)^{0.25}|\Delta\varphi_0|, \tag{13}$$

for

$$|\Delta\varphi_0| < \pi, \tag{14}$$

where $\Delta T_{\text{p-v}}$ denotes the peak to valley normalized transmission difference in the Z-scan curve, which can be directly calculated from the data. Therefore, Eqs. (13) and (14) can be used directly to calculate the nonlinear refraction coefficients. With the Z-scan technique and equations summarized in this section, the nonlinear performance of a system can be quantitatively characterized and benchmarked with other systems, which offers convenient ways and standards to evaluate the optical nonlinearities for different materials and design new devices.

Laser ablation to synthesize nanoparticles

Laser ablation to produce nanoparticles has developed into an important field. It is known as a green, efficient, and universal physical approach for nanoparticles' generation, versatile for fast one-step synthesis and potential mass production. It is a flourishing research direction widely applied in biology, chemistry, optics, materials science, and many other research fields. Various types of materials are available, including semiconductors, metals, organics, and hybrid composites. Based on high power lasers, many other techniques are developed. For example, for nanoparticles in liquid, laser fragmentation can be used to further reduce the nanoparticles' sizes. On the other hand, laser melting method can heat metallic nanoparticles until they are melted and combined together to form larger particles. Other techniques can also be used for defect engineering and modification of optical properties[31]. Different reviews were published to summarize the physics behind, various types of materials, the influence of different experimental factors, applications, and challenges[23–33].

Laser ablation has proven to be a successful approach for nonlinear optical nanoparticles' synthesis due to the following advantages[28,38,39]. **For purity:** Most of the applications require nanoparticles to have specific surface activities without any residual chemical precursors. For other synthesis methods, this requires complicated treatments and cleaning. Laser ablation is a direct physical approach fundamentally different from chemical methods. It produces nanoparticles with high purity, which

facilities the direct use of nano-products for optical applications in medical, chemical, biological, and biochemical fields. In addition, the products do not contain any capping ligands on their surfaces, favorable as the reactants for further modification or processing. Due to its straightforward process without any requirement for post-processing, laser ablation for nanoparticles' synthesis can be conducted automatically. This process can be optimized to provide great potential for the scalable production of nanoparticles. **For flexibility:** Laser ablation is a versatile approach to synthesize nanoparticles by demands, which can be widely applied to almost all materials, ranging from metals, dielectrics, to polymeric materials with proper laser ablation parameters. Even nanoparticles of complex multi-elements or alloys can be synthesized freely. Highly flexible combinations of target materials and the surrounding matrices can be considered to make different functional devices. Nanoparticles can be synthesized in most solutions of choices. Laser ablation is capable to produce nanoparticles with various properties, including structures, compositions, sizes & size distributions, and concentrations inside a solution. A variety of laser processing parameters allow great flexibility in the nanoparticles' production, which includes laser fluence, pulse duration, repetition rate, and light wavelength. The electroaffinity and defects of the nanoparticles can be controlled. Many laser ablation processes do not require special experimental conditions or post-treatments. The process can be conducted at room temperature and in ambient air. **For operation**: Laser ablation does not require a long reaction time. It is a single-step synthesis which can be completed in a short time. Laser ablation is highly efficient, sustainable, and environmentally friendly, which is compatible with the principles of environmental-friendly synthesis[40]. Different from the conventional chemical process, minimal manual operation is involved. It does not require pyrophoric, hazardous, or toxic chemical precursors. The substrate materials for laser ablation are often several times cheaper than the compounds used in the chemical processes. Furthermore, it does not involve critical safety issues. Laser ablation can provide a localized high-pressure and high-temperature environment at the laser focal spot. Such a condition is favorable for many materials which require localized extreme conditions, such as for the synthesis of cubic boron nitride nanoparticles[39,41–43].

Nanoparticles' synthesis experimental setup

To design the synthesis experiment and select proper parameters, the experimental setup and its operation process are revisited. Laser ablation experimental setup can be highly flexible to address various demands of nonlinear optical nanoparticles. It primarily consists of two key subsystems: the optical system and chamber to host the substrate (Fig. 3). The optical system involves two parts: laser source and optics to modulate laser beam (Fig. 3(a)). For the selection of optical components, a balance needs to be kept between the long working distance and high laser fluence, as an optical lens with a large numerical aperture (NA) can increase the laser fluence but sacrifices the working distance. During the operation, a Galvo scanner is typically used to constantly change the position of the focal point to ensure full interaction with the substrate surface, which maintains the uniformity in the nanoparticles' fabrication. Chamber design highly depends on matrix selection. For vacuum, a sealed chamber is required to connect to a pump to remove the gas out. For the gas matrix other than air, the substrate is put into a sealed chamber with a flat transparent glass window to transmit laser in. Pipes are connected to the chamber as the supply/outlet of selected gases to provide the proper matrix. For the liquid matrix, the substrate is immersed inside a liquid container and a heating plate may be used to control the temperature.

Customized chamber design can also be considered to meet requirements for specific nonlinear systems or extend functionalities. For example, as direct laser ablation normally synthesizes nanoparticles with a wide size distribution, it is a primary challenge to produce or select nanoparticles with similar sizes, as shown in Fig. 3(b)[44]. However, for optical nonlinear applications, particle size is a critical parameter to affect the device performance, such as surface plasmonic resonance peak. Different from conventional designs, the substrate is put in a vertical direction and laser irradiates at an angle of ~45 degrees to the horizontal direction. Since laser ablation is a dynamic process of rapid removal of target materials, a recoil pressure is generated and acts on the target when the species leave the surface. The evaporated atoms and plasma species form nanoparticles in ambient air during its dynamic process flying away from the target. Due to the gravity force, nanoparticles eventually land on collectors. Different sizes of nanoparticles are ejected from the target at different speeds. Thus, the distance between the target and the landing point of the nanoparticles on

the substrate is different for different sizes of nanoparticles. Large nanoparticles are close to the target and the size distribution shifts towards smaller nanoparticles at a longer target –substrate distance. Hence, nanoparticles of various sizes are separated nicely. Consequently, holes in the collectors can be used to separate and collect nanoparticles at different sizes[45]. Furthermore, other chamber designs can also be considered. For the liquid matrix, multiple substrates can be used for the synthesis of alloys or hybrid nanoparticle compounds[46,47]. Substrates are immersed inside the liquid. To further control the morphology of the nanoparticles synthesized, a couple of electrodes can also be applied on two sides of the liquid tanks to apply a DC electric field[48]. In some cases, the laser ablation can trigger the undesired reactions between the substrate materials and liquid. To avoid undesired reactions, the substrate can be firstly ablated inside the chamber with a continuous gas flow. The gas flow then carries the synthesized nanoparticles out. The gas flow can then be guided to mix with the liquid to prepare the solution of the nanoparticles. Additional cases of more customized chamber designs for more specific purposes can be referred in the literature[26,27,48]. For example, carbon nanoparticles can be synthesized in vacuum[49].

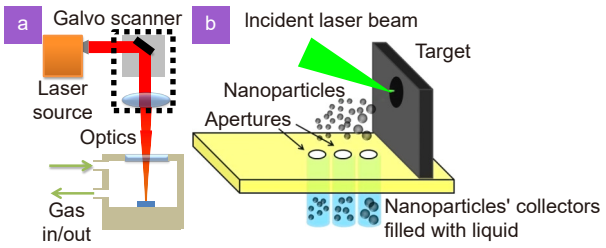

Fig. 3 | Experimental setups. (**a**) Laser ablation inside a vacuum chamber for selected gas matrix. (**b**) Laser ablation with the size selection of nanoparticle synthesis in air.

Optimization of experimental factors for different nanoparticles' synthesis

Once the experimental setup is constructed, proper parameters need to be determined to produce desired nanoparticles. Many parameters affect the properties of the nanoparticles synthesized, including laser pulse duration, wavelength, repetition rate, and laser fluence[50]. i) **Pulse duration** affects laser peak intensity as well as ablation mechanism. Many types of materials can be processed by lasers with both short and long pulse durations. However, some materials are sensitive to the thermal effect so they prefer lasers with short pulse duration. ii) **Wavelength** is closely related to absorption coefficients, which need to be selected properly based on the absorption spectrum of the target. The wavelength selection is also determined by the absorption of liquid. For a pulsed laser with high peak power, it is necessary to consider the nonlinear effects of the system in nanoparticles' synthesis[40]. iii) **Repetition rate** determines the number of laser pulses in a unit time. Generally speaking, productivity increases linearly with the repetition rate[51]. In certain cases, it is also reported that the repetition rate can affect the nanoparticles' sizes. When the repetition rate is increased, nanoparticles produced have smaller sizes and narrower size distributions[52]. iv) **Laser fluence:** A lot of research efforts are devoted to exploring the relation between the laser fluence and morphologies of nanoparticles[50]. For every type of target, there is a threshold to trigger the laser ablation, which should be the minimum value of laser fluence required to remove the target material. In the liquid matrix, laser beam needs to penetrate the liquid layer to reach the target surface. Laser fluence should not be too high to avoid the nonlinear effects and breakdown of the liquid. In the air, an increase of laser fluence leads to an increased density of atoms in the plasma, which results in increased sizes of the nanoparticles. Laser fluence also influences the nanoparticles' structure[53]. Higher laser fluence results in nanoparticles with smoother surfaces and less irregular shapes[54]. It also affects the size distribution. Furthermore, laser fluence is also related to photothermal reshaping and fragmentation[55].

For the chamber sub-system, the matrix and substrates are two important selections. The gas system has been explained in the previous section. The type of gas in the chamber can be flexibly controlled by pumping the desired gas. The pressure of the environment can also be tuned with the pumping system. For materials being easily oxidized, protective gas is required. Liquid matrix is also widely used. Common choices of the liquid matrices are presented in Table 1. The choices of the matrix affect the expansion velocity, lifetime, nucleation, crystal growth mechanism, and final structure of nanoparticles. For example, in the steam environment, the ablation performance is enhanced by more than 100% compared to the synthesis efficiency in ambient air for certain cases[56]. The thickness of the liquid layer certainly affects the confinement of the plasma plume expansion[26]. If the expansion of the plasma plume is more compressed by the

Table 1 | Common liquid matrices for laser ablation.

No.	Liquid	Material	Note
1	deionized water	Au[59], Co[57], Ag[60], Ti[61], Al[61], Si[62], ZnO[63], Quantum dots (CdTe, CdSe, ZnTe)[64,65], Carbon-based materials[66], Oxo(phthalocyaninato)vanadium[67], Alloys[68]	Most popular liquid matrix
2	n-hexane, diethyl ether, toluene, 2-propanol, acetone, and methanol	Au[57], Co[57], Alloys[69]	Relatively stable organic matrices
3	ethanol	Al[70], Ti[61], ZnO[63]	Al slowly reacts with oxygen[70]
4	chloroform, carbon tetrachloride, dichloromethane, cyclohexane	Al[71]	Organic matrices with different polarities and densities
5	wax	Si[72]	Phase change matrix

liquid matrix, nanoparticles with smaller diameters are produced due to the reduced time of nucleation and growth. It is also demonstrated that the polarity of the liquid molecules can affect the size distribution of nanoparticles[57]. Self-focusing and optical limiting are also related to the final laser energy reaching the target surface. When the incident energy exceeds the nonlinear threshold of the liquid, nonlinear effects need to be considered[58]. For further modification or size control purposes, surfactant or reaction agents can also be added into the liquid to manipulate the nanoparticles' synthesis[31].

Nonlinear optical nanoparticles' production, functions, and applications

Nonlinear optical nanoparticles' production

Nanoparticles are the fundamental building blocks for many nonlinear optical systems. Table 2 benchmarks the sizes of nanoparticles with different micro/nano-systems. In this section, several representatives are selected to demonstrate how to produce nanoaprticles with desired optical properties. The composition and morphology are two important features to determine the functionalities of nanoparticles. Among the great variety of nanoparticles available by laser ablation, three categories of materials are selected as the representatives widely used in nonlinear optical systems, which introduces the methods and experimental results and demonstrates how to engineer the desired composition and morphology. These case studies cover: 1) carbons and organics 2) metals and oxides, and 3) semiconductors and dielectrics.

Carbon based materials

Many types of carbon-based materials can be prepared by laser ablation as demonstrated in Fig. 4(a) to 4(c), which are representatives to show how laser ablation can engineer different compositions of the nanoparticles produced from the same type of substrate[30,66]. By changing experimental conditions, carbon nanoparticles fabricated have features that are different from each other (Figs. 4(a) and 4(b)). Carbon nanoparticles can be fabricated inside a vacuum chamber. In the experiment, a KrF excimer nanosecond laser with a wavelength of 248 nm and pulse duration of 23 ns was used to ablate the carbon plate. The laser fluence and repetition rates were 3.2 J/cm^2 and 10 Hz, respectively. Nanoparticles fabricated had an average diameter of 20 nm. The sizes were relatively uniform. It was found that the size depends on the vacuum pressure. For a relatively low gas pressure, nanoparticles with smaller diameters could also be fabricated. An increase in gas pressure led to a large average size and size distribution[73]. While for the laser ablation in water, carbon nanoparticles with a wider size distribution and different morphologies could be fabricated as demonstrated in Fig. 4(b). In the experiment, a carbon plate was ablated by the nanosecond laser at the wavelength of 532 nm. The repetition rate and laser fluence were measured to be 10 Hz and 0.8 J/cm^2, respectively. The size of the nanoparticles ranged from 10 to 20 nm. Carbon nanoparticles with different features are used for various nonlinear optical applications. For example, nanoparticles ablated in liquid demonstrated superior optical limiting performance compared to the benchmark materials, such as C_{60}, which is a common benchmarking material for optical limiting performance[74,75]. More details will be covered in the later section on the nanoparticles' applications.

One interesting topic is the synthesis of nano-diamonds (Fig. 4(c)). Nano-diamonds are reported to have nonlinear responses in the near-infrared wavelengths[76]. The fabrication often involves extreme conditions, such

Table 2 | Nanoparticles' size comparison.

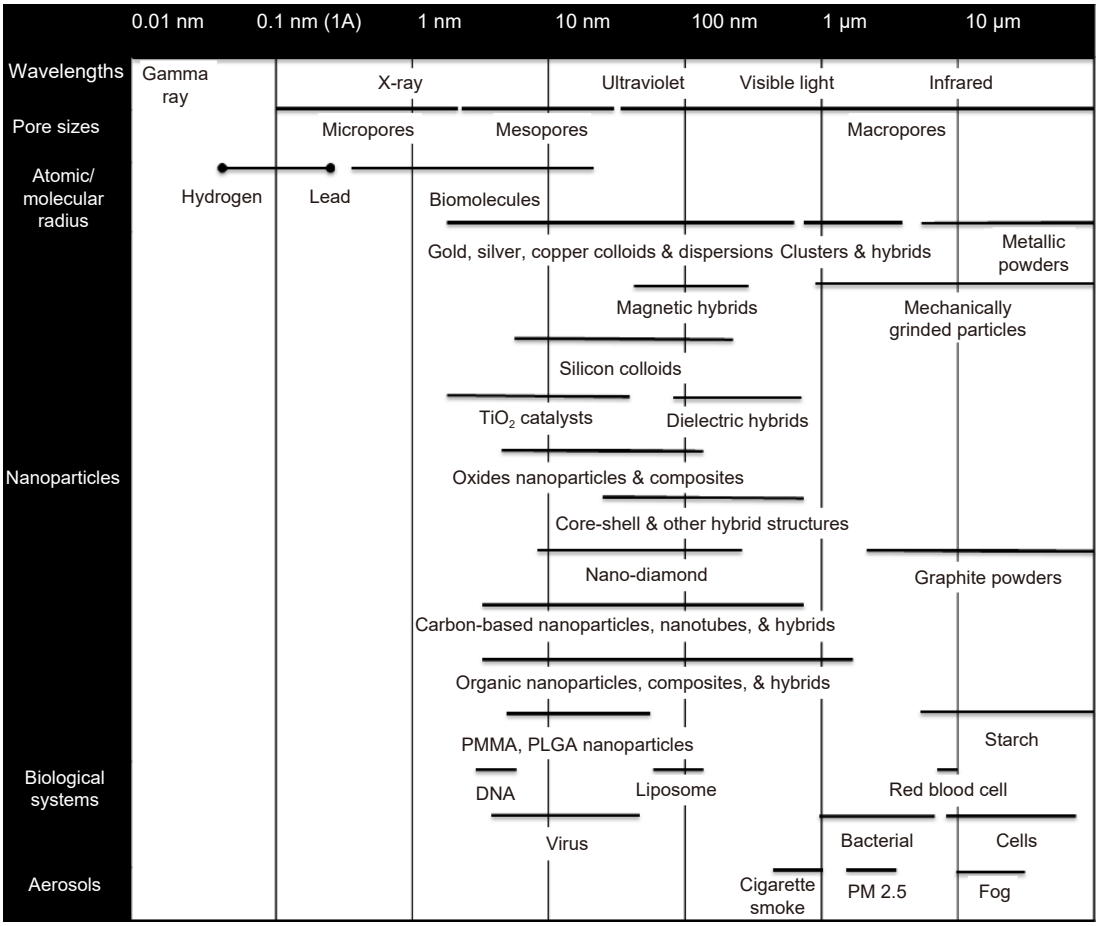

as high temperature and high pressure, which is challenging for most other techniques in ambient conditions. Laser ablation to produce various types of nano-diamonds has a long history and is summarized in the reference[77]. In previous studies, focused laser beam provides the desired extreme experimental conditions that are critical for diamond formation. The synthesis of nano-sized diamonds is often conducted in liquid. High temperature and high pressure are generated in the expansion process of plasma plume. For the case of diamond synthesis, the temperature and pressure are in the range of 4000 to 5000 K and 10 to 15 GPa, respectively[78]. The laser-induced plasma contains the energetic species ablated from the carbon-based substrate, including the clusters with sp^2 bonding, electrons, and ions. In the plasma plume, the condition is suitable for the formation of diamonds. For this condition, the diamond phase with sp^3 bonding is more stable than the graphite phase with sp^2 bonding. Hence, the formation of diamond nuclei is preferable to that of graphite inside a plasma. Subsequently, the diamond nucleation takes place and grows from the phase transition. It is also reported that inside water, there is a sufficient supply of OH^- and H^+ ions to maintain the incorporation and diffusion mechanisms, which promotes the growth of diamond nuclei by suppressing graphite sp^2 bonding[79]. The shockwave in the ablation also affects the generation of nano-diamonds[80,81]. Nano-diamond with different properties can be synthesized and deposited on a flat metallic substrate, such as copper. However, the primary limitation is the size of the diamond synthesized. Due to the limited time of plasma plume expansion and condensation, most diamonds synthesized only had sizes from tens to hundreds of nanometers[78]. Although many experiments have been conducted, the synthesis process is still not fully understood due to its complexity, which makes it challenging to further increase the size[77].

Metals & oxides

Metallic and oxide nanoparticles have extensive applications for nonlinear optics as well as many other functional devices[32]. Morphology is critical to determine the properties of the metallic nanoparticles, such as the resonance wavelength for nonlinear absorption[82]. Three

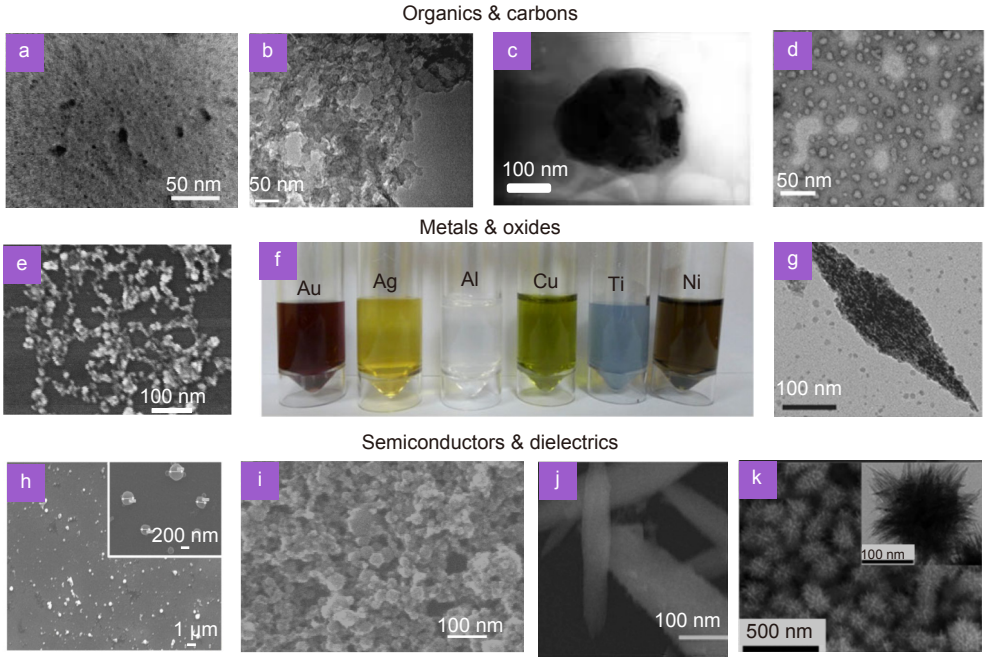

Fig. 4 | Nanoparticles synthesized by laser ablation. (**a**) TEM image of carbon nanoparticles synthesized with an average size of 6.5 nm. (**b**) TEM image of carbon nanoparticles fabricated in liquid. (**c**) TEM image of nano-diamond particles fabricated by laser ablation. The diamond nanoparticle was measured to have a grain size ~300 nm. (**d**) TEM image of organic particles fabricated in water. (**e**) SEM image of the Co nanoparticles synthesized. (**f**) Optical images of various metallic nanoparticles' dispersions. Colors of Au, Ag, Al, Cu, Ti, and Ni nanoparticle dispersions are dark red, orange, transparent, dark green, blue, and dark yellow, respectively. (**g**) SEM image of CuO nanospindles. (**h**) SEM image of silicon nanoparticles synthesized in water. Most nanoparticles were around 100 to 300 nm. Some were below 100 nm. (Inset: zoom-in SEM image). (**i**) SEM image of TiO_2/Ag hybrid nanoparticles. The size ranged from 20 to 30 nm. (**j**) SEM picture of GeO_2 nano-rods synthesized in water. (**k**) SEM picture of the urchin-like $ZnSnO_3$ nanoparticles. Inset: zoom-in picture of a single urchin-like nanoparticle[58,62,73,74,120–122]. Figure reproduced from: (b) ref.[74], American Institute of Physics; (c) ref.[120], Springer-Verlag; (d) ref.[121], Elsevier; (e) ref.[122], Elsevier; (h) ref.[62], under a Creative Commons Attribution 3.0 License.

examples demonstrate how laser ablation can produce a variety of Au nanoparticles with different morphologies, as demonstrated in Fig. 4(f). Different colors in the figure are attributed to different surface plasmonic properties[83]. Many efforts are devoted to produce Au nanoparticles with desired sizes and shapes[84]. Gold nanoparticles were fabricated with a nanosecond laser at a wavelength of 1064 nm. A gold substrate was immersed inside water during the ablation. The repetition rate and laser fluence were set as 100 kHz and 12.5 J/cm^2, respectively. The diameters of the gold nanoparticles were in a range from 5 to 30 nm. The color of the dispersion reflected the plasmonic properties of nanoparticles, indicating the capability to engineer and shift the absorption peaks for nonlinear applications. Reshaping and fragmentation of Au nanoparticles were also widely studied for size modification[32]. For example, it was reported that 800 nm femtosecond pulsed laser could reshape anisotropic Au nanoparticles into spherical shapes[85]. On the other hand, nanosecond laser pulses resulted in the fragmentation of Au nanoparticles[86]. Fundamentally, the electron dynamics of nanoparticles and the relaxation processes after the laser irradiation were reported to be the mechanisms to govern both the reshaping and fragmentation phenomena[87]. The key parameters to determine the processes are both the laser parameters and material properties[88,89].

Furthermore, the morphology of the nanoparticles is not limited to spherical shapes. Many factors can change the shape of the nanoparticles, including the addition of surfactants and applying external electric fields[90]. SEM image of the CuO nanospindles is shown in Fig. 4(g), which also demonstrates controllable nonlinear optical responses depending on their shapes[91]. For the laser ablation synthesis of nanoparticles, a nanosecond laser at a wavelength of 532 nm was used to ablate the copper target inside water. The repetition rate and pulse energy were 5 Hz and 100 mJ, respectively. To control the shape of the nanoparticles synthesized, a couple of copper foil electrodes were fixed on the walls of the liquid tank. A

DC electrical field with an adjusting voltage was applied. It was found that the shape of the nanoparticles depended on the strength of the electric field applied. As the electric field increased, nanoparticles changed from nano-rods to nanospindles as demonstrated in Fig. 4(g). The aspect ratio could be flexibly controlled, which demonstrated the capability to engineer the morphology of the nanoparticles synthesized by laser ablation.

Semiconductors and dielectrics

Laser ablation is also a powerful tool to synthesize semiconductor and dielectric nonlinear optical nanoparticles. Many types of nanoparticles are available, including silicon, silica, germanium and its oxides, phase change materials, and dielectric oxides[62,72,92–94]. Among them, silicon is a widely used nonlinear semiconductor material with a number of applications[62]. Figure 4(h) shows the silicon nanoparticles synthesized by laser ablation inside water. The pulse duration and wavelength of the Nd:YAG laser used in the experiment were 1.5 ns and 1064 nm, respectively. The repetition rate was 60 kHz and the laser fluence was measured to be 0.8 J/cm^2 at the focal point. For the SEM characterization, the dispersion of the silicon nanoparticles was dropped onto an undoped silicon substrate. The Si nanoparticles were mostly spherical. The size distribution ranged broadly from 5 to 400 nm, while most of the nanoparticles had a diameter of 100 to 200 nm. Silicon wafers with different doping types and concentrations were ablated by the same experimental setup. The size distributions were reported to be similar for silicon substrates with different doping concentrations[62,95]. The addition of dopants is required to achieve tunable optical nonlinear functions, which may be challenging for other nanoparticle synthesis methods. The details of their nonlinear performance will be discussed in the next section. However, for laser ablation, various morphologies and compositions of silicon nanoparticles can be synthesized as it is highly flexible to select different substrates[96]. For the improved control and production of selective sizes of nanoparticles with a more uniform distribution, the experimental setup discussed in the previous section can be considered[62,72].

Dielectrics are also important optical nonlinear materials for many devices[97]. Many dielectric nanoparticles are synthesized by laser ablation (Fig. 4(i)). TiO_2 nonlinear nanoparticles could also be synthesized by Nd:YAG nanosecond pulsed laser with a 1064 nm wavelength. The repetition rate was 10 Hz. A titanium metal plate was used as the substrate inside DI water. TiO_2 has a relatively high refractive index. The nanoparticles produced were characterized by SEM and presented in Fig. 4(i). The size of the TiO_2 nanoparticles ranged from 20 to 30 nm. Ag deposited TiO_2 nanoparticles could also be fabricated to enhance the optical performance. To achieve this objective, a silver plate was subsequently put into the TiO_2 nanoparticles solution and ablated by the same laser. Ag nanoparticles synthesized were measured to have an average diameter of 10 nm[92]. Laser ablation demonstrated the flexibility to further decorate TiO_2 nonlinear nanoparticles with different metallic nano-materials. Huge potentials can be explored as laser ablation can be applied to synthesize hybrid materials and alloys for hybrid nonlinear systems. For example, this TiO_2 experiment only demonstrates the process with a two-step laser ablation. More laser ablation steps can be used to add different materials in the composites to fabricate more complicated nanoparticles based on three or more materials, which can meet demands for different multifunctional devices.

Many functional devices demand nonlinear optical nanoparticles to have different shapes. Similar to metals and oxides, nanoparticles other than spherical shapes are available. GeO_2 based hybrid system has also been proven to be a good candidate for nonlinear devices[98]. Figure 4(j) is the SEM image of the GeO_2 nano-rods synthesized by laser ablation[99]. A nanosecond laser at a wavelength of 532 nm was used to ablate the Ge substrate inside water. The repetition rate and pulse energy were 5 Hz and 150 mJ, respectively. An external electric field was applied through a couple of DC electrodes placed at both sides of the liquid tank. Similar to the synthesis of oxide nanoparticles, the external electric field is proved to be effective to control the morphology of nano-rods. Figure 4(k) is the SEM image of another example to demonstrate urchin-like $ZnSnO_3$[100]. A nanosecond laser at a wavelength of 1064 nm was used to ablate a zinc plate inside water. The repetition rate and pulse energy were 10 Hz and 100 mJ, respectively. In this process, the colloidal solution of $ZnO_x(OH)_y$ was produced. The same laser ablation experimental conditions were applied to prepare SnO_x precursors. These two precursors were then mixed at a volume ratio of 1∶1. A strong ammonia solution (28%) was added and the mixture was heated up to 180 °C for 15 hours. The product was collected, centrifuged, and washed with DI water. The collected nanoparticles proved to be useful with high

photocatalytic activity for waste reduction. Depending on the applications, laser ablation is a versatile method to produce nanoparticles with various desired shapes.

Nonlinear optical nanoparticles' performance

The performance of the nanoparticles is based on many factors. In this section, concepts and demonstrations to achieve various types of functions are introduced. We shall begin with the most fundamental systems which involve nanoparticles directly mixed in different matrixes. Secondly, more complicated systems based on hybrid components are introduced. The functionalities and the performance are further enhanced. Finally, the discussion continues from static to dynamic nonlinear optical systems with rich mechanisms and physics to achieve superior properties, such as tunable nonlinearity and self-healing.

Nonlinear optical nanoparticles inside different matrices

Various types of systems based on nonlinear optical nanoparticles have been proposed. The most basic type is to mix the nanoparticles inside transparent liquids to form a solution with optical nonlinearity. The performance of this nonlinear system primarily depends on the type of nanoparticles[75]. Hence, three examples are selected for different categories of materials. The first case is carbon nanoparticles. Carbon nanoparticles with the average sizes ranging from 3.5 to 6 nm are prepared. No addition of any surfactant is required as the carbon nanoparticles are self-stabilized in liquid. Raman characterization shows that the carbon nanoparticles in tetrahydrofuran are amorphous in carbon bondings, which demonstrates the presence of polymerization during nanoparticles' formation. The transmittance of the prepared sample was measured with a Q-switched Nd:YAG laser. The wavelength is 532 nm with the laser pulses of nearly Gaussian profile and 7 ns pulse duration. The laser beam was focused into the sample by a focusing mirror at a focal length of 25 cm. The thickness of the sample was measured to be 1 cm. The results are presented in Fig. 5. The transmittance begins to decrease at a laser fluence of 0.3 J/cm^2 and becomes nearly 33% of the initial value at 10 J/cm^2. It demonstrates an excellent optical limiting behavior. The nonlinear performance of carbon nanoparticles inside water is also plotted as the reference. It is found that the size of the nanoparticles plays an important role. When the size is less than 3.5 nm, the nonlinearity disappears and no optical limiting behavior is observed for the laser fluence up to 10 J/cm^2. This is due to the nonlinear scattering induced by the carbon nanoparticles. Larger nanoparticles with a bigger absorption cross-section can form solvent bubbles more effectively than smaller nanoparticles. Hence, the nonlinear scattering performance is enhanced[75].

Silver nanoparticles are selected as an example of metallic materials. Silver nanoparticles can also be prepared in the polymethyl methacrylate (PMMA) film. The silver metal foil is ablated in tetrahydrofuran to obtain the nanoparticles. Purified PMMA is added and mixed together. The mixture is then cast on a 70 mm diameter petri dish to produce a film with 0.18 mm thickness after drying. The sizes of the nanoparticles range from 15 to 30 nm in diameter. Most of the nanoparticles are spherical. As a reference, silver nanoparticles in water are also fabricated. Sulfosuccinate is added into the water matrix as the surfactant to stabilize the silver nanoparticles and help them better disperse in water. Otherwise, silver nanoparticles tend to reside around the ablation spot, absorb the incident laser pulses, and decrease significantly the yield of the final product. The same 532 nm pulsed laser is used for the measurement of optical nonlinearity. To reduce the average power, the laser is set to operate in the single-shot mode. A combination of half waveplate and polarizer is used to control input laser fluence. A lens with the focal length of 25 cm is used to focus the incident laser beam to the center of the quartz cuvette with a 1 cm optical length, which contains the sample, as shown in Fig. 5(b). Silver nanoparticles demonstrate optical limiting in both the PMMA film and water. As a reference, both pure water and PMMA do not demonstrate any nonlinear behaviors. Silver nanoparticles in water exhibit nonlinear transmission at the threshold of 0.4 J/cm^2. For PMMA film containing silver nanoparticles, the threshold is slightly higher (0.6 J/cm^2). It is reported that the nonlinear absorption of silver nanoparticles in the nanosecond time scale is due to the photoinduced formation of electron hole pairs that offer strong free-carrier absorption. Meanwhile, other mechanisms associated with the interaction between the nanoparticles and the matrix can be responsible for the enhanced optical limiting behavior of silver nanoparticles suspended inside an aqueous solution.

Semiconductors are also functional materials for nonlinear optical devices. Silicon nanoparticles with different doping concentrations are demonstrated as an

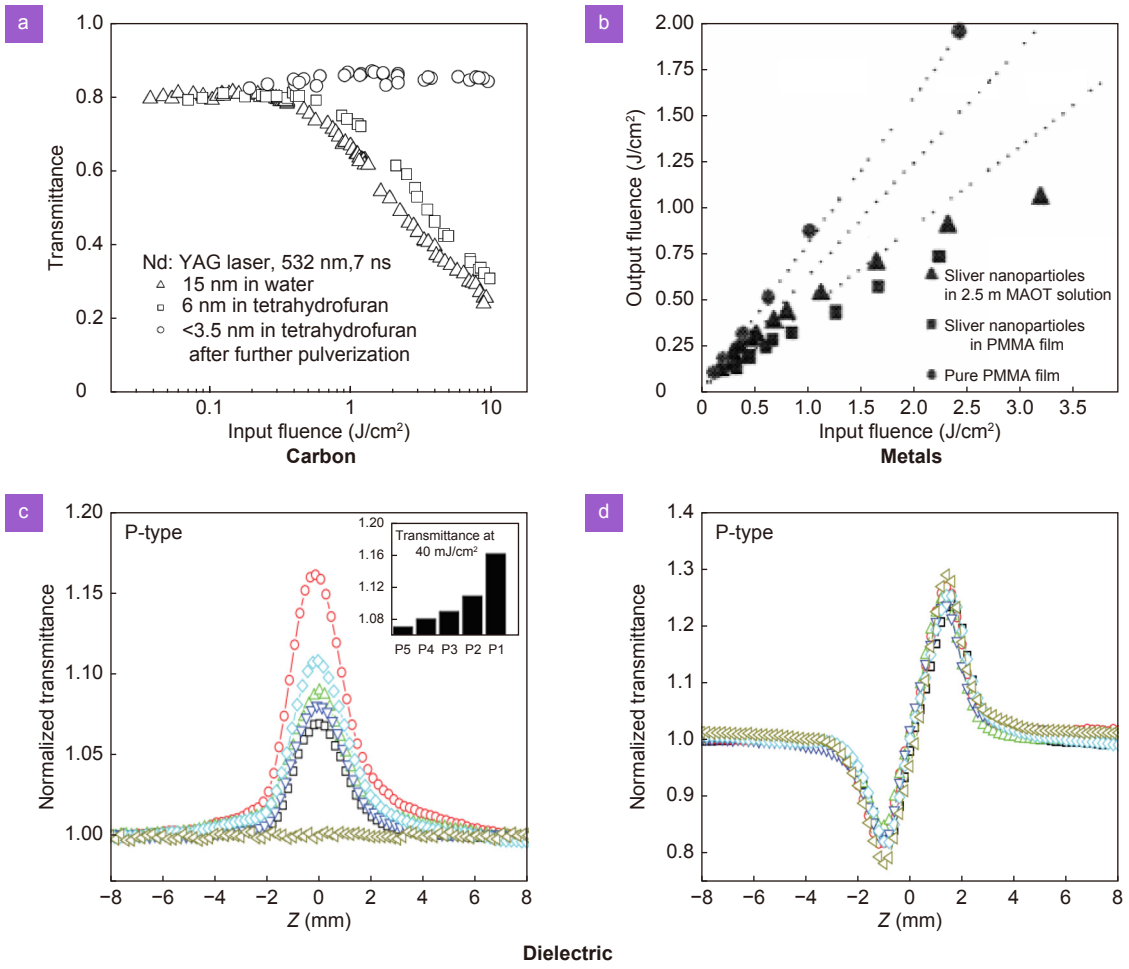

Fig. 5 | Optical nonlinear characterization for (**a**) carbon nanoparticles, (**b**) metallic nanoparticles, (**c**) open aperture and (**d**) close aperture Z-scan results for dielectric nanoparticles[62,75,123]. Figure reproduced from: (a) ref.[75], IOP Publishing; (b) ref.[123], SPIE; (c) ref.[62], under a Creative Commons Attribution 3.0 Licens.

example of the cost-efficient, highly flexible, and low toxic candidates. Detail fabrication process is discussed in the previous section. The silicon nanoparticles fabricated by laser ablation have the size distribution ranging from 10 to 400 nm, with the distribution peak located at 100–200 nm. Such size distribution is similar for silicon wafers at different doping types or concentrations. To characterize the nonlinear optical responses, both open and close aperture Z-scan experiments are conducted. The setup and experimental procedure are introduced in the previous section. The results are summarized in Figs. 5(c) and 5(d). All the P-type silicon nanoparticles with different doping concentrations demonstrate features of saturable absorption. Comparing the curves for different samples, the peak transmittance increases with doping concentration, which indicates that the saturable absorption is enhanced by the dopants. The enhanced nonlinear performance is attributed to the mechanisms of free carrier absorption, which is discussed in detail in the previous sections of nonlinear mechanisms. The dopants increase the number of free carriers in the materials and promote the nonlinear behaviors. For the close aperture Z-scan, all the samples demonstrate self-focusing features with similar peak transmittance. As the concentration of the silicon nanoparticles in water is relatively low, the effect of doping concentration is not as obvious according to the open-aperture Z-scan measurement.

Nanoparticles for hybrid nonlinear optical systems

The previous examples are based on pure nanoparticles in various matrixes. Nonlinear optical nanoparticles can also be further developed into hybrid systems to further extend the functions. Different from the conventional process on the bulk substrate, laser ablation can be applied directly to the hybrid systems to further modify the properties. For example, nanoparticles can be deposited to form thin films. One good example is the nonlinear devices based on graphene oxide. Graphene oxide is

widely used in many applications, including integrated photonic devices, flat optics, ultrafast laser systems, fluorescent materials for bio-imaging, and bio-sensing[101,102]. It is reported that a laser ablation can process and modify the optical properties of graphene oxide (GO) nanoparticles[103]. To characterize the nonlinearity, GO nanoparticles are firstly spin-coated to produce a thin film. With the continuous irradiation of the laser beam, the GO nanoparticles undergo four stages of different nonlinear optical activities. Without the reduction process induced by laser, the GO nanoparticles show a typical saturable absorption. When the laser fluence increases from 15.9 to 32 J/cm^2, the nonlinear performance of the partially reduced GO solution converts into the optical limiting behavior. This process is found to be reversible if the incident laser irradiation is removed. If the laser fluence is further increased from 32 to 50 J/cm^2, the chemical reduction of GO nanoparticles is triggered by high laser intensity. The optical limiting performance is enhanced. 50 J/cm^2 is the second threshold for the GO nanoparticles to be fully reduced. At this point, the optical limiting effect reaches its maximum value. This transition process is attributed to different properties of the GO and reduced GO nanoparticles. Saturable absorption is observed for GO because its ground-state can be saturated easily because of its band structure. For the reduced GO, the two-photon absorption and excited-state absorption of its sp^3 bonds are responsible for the optical limiting performance[103].

The thin film formed by the laser ablated GO nanoparticles can be further upgraded to enhance its performance. As demonstrated in Fig. 6, silica microspheres are deposited on the prepared GO thin films. A direct drop-casting method is used to control the density of the silica microspheres on top of the thin films. Microsphere dispersions with different concentrations are dropped on the GO films and transferred to a hot plate until water is fully evaporated. An optical microscope is used to accurately measure the average coverage of silica microspheres on the GO film. The function of the microspheres is to serve as a particle lens. Such particle lens can focus incident light and produce local field enhancement at the bottom of the lens, which is shown in Fig. 6(b). This local field enhancement is also denoted as the photonic nanojet (PNJ). The silica microspheres used have a diameter of 1 μm. For this size, the PNJ enhances the light intensity by more than 8 times compared to the incident light without microspheres. The enhanced light can propagate for a distance of more than 400 nm from the bottom surface of the microsphere into the matrix. The Z-scan measurement is carried out for the GO with microspheres. A femtosecond pulsed laser at the wavelength of 800 nm is used as the light source. The pulse duration and repetition rate are 50 fs and 1 kHz, respectively. The results are summarized in Fig. 6(c) to 6(f). As the reference group, the GO film demonstrates saturable features similar to the one presented in the previous case. When the microsphere is added on the film, its nonlinear performance is enhanced by more than 33% compared to the reference group. The optical image of the GO film and GO + microspheres are shown in Fig. 6(e). The coverage of the microsphere on the GO film is relatively low (10%). It demonstrates that this method still has great potential if a compact layer of the microspheres can be formed. Furthermore, the enhancement of the microspheres is not limited to a specific type of nonlinear material. It is a highly versatile and flexible approach that can be considered in many different nonlinear systems.

Nanoparticles for dynamic nonlinear optical systems

In the previous cases, static nonlinear optical systems are presented. Many important applications require dynamic responses. Hence, it is demanded to further develop the nanoparticles and make them suitable to construct dynamic devices, which can respond differently based on different conditions. One strategy is to integrate the nanoparticles of phase change materials. Two examples are presented. Figure 7 demonstrates the first dynamic system based on GO nanoparticles processed by laser ablation. It contains the frozen matrix based on ice, which preserves the advantages of the liquid system but also fulfills the requirements of solid-state devices. GO nanosheets with diameters ranging from 300 nm to a few microns are mixed inside water. The concentration is 5 g/L. Silica microspheres are added into the GO dispersion. The diameter of microspheres is 1000 nm. The number of microspheres per unit weight is 8.2 ×10^9 g^{-1}. The fabrication of the frozen matrix is demonstrated in Fig. 7(c) and 7(d). A cell made of optical glass is used as the container. The optical path length of the cell is 1 mm. The dispersion is carefully injected into the cell to avoid any bubble formation. It is then transferred into an enclosed cold environment cooled by dry ice and freezes within half a minute. Similar to the hybrid system presented previously, the silica microspheres serve as the particle

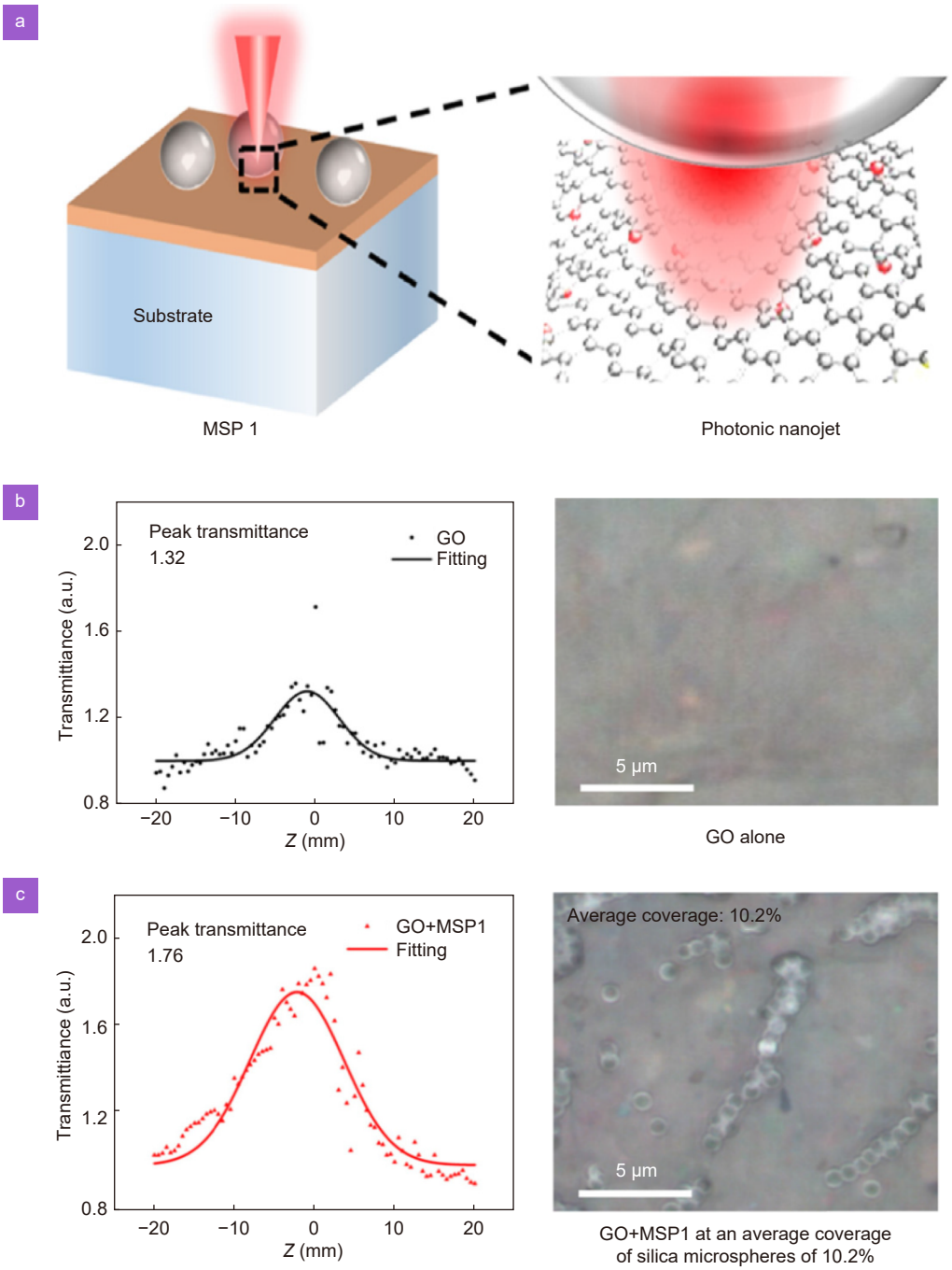

Fig. 6 | Hybrid nonlinear optical systems based on nanoparticles. (**a**) Schematic diagram to demonstrate the GO system hybridized with transparent microspheres. The photonic nanojet can cause the enhancement of optical nonlinearity. (**b**) and (**c**) Nonlinear optical characterization and optical images of the reference group of pure GO and the GO+microspheres sample. Figure reproduced with permission from ref.[124], Optical Society of America.

lens in the frozen matrix. A local field enhancement is introduced due to the focusing of the microspheres. In the frozen matrix, the area of local field enhancement is calculated to be around 1.01 μm^3. It is 1.9 times the volume of the microsphere. GO nanoparticles presented in this volume have enhanced nonlinear performance. The nonlinear absorption of the frozen sample is characterized at the wavelength of 800 nm with a femtosecond laser (100 fs pulse duration, 1 kHz repetition rate). The output laser fluence versus input laser fluence for different samples is presented in Fig. 7(b). Without the GO nanoparticles, the frozen matrix and silica microspheres do not demonstrate any nonlinear response. The black line is a reference for the linear transmittance of the

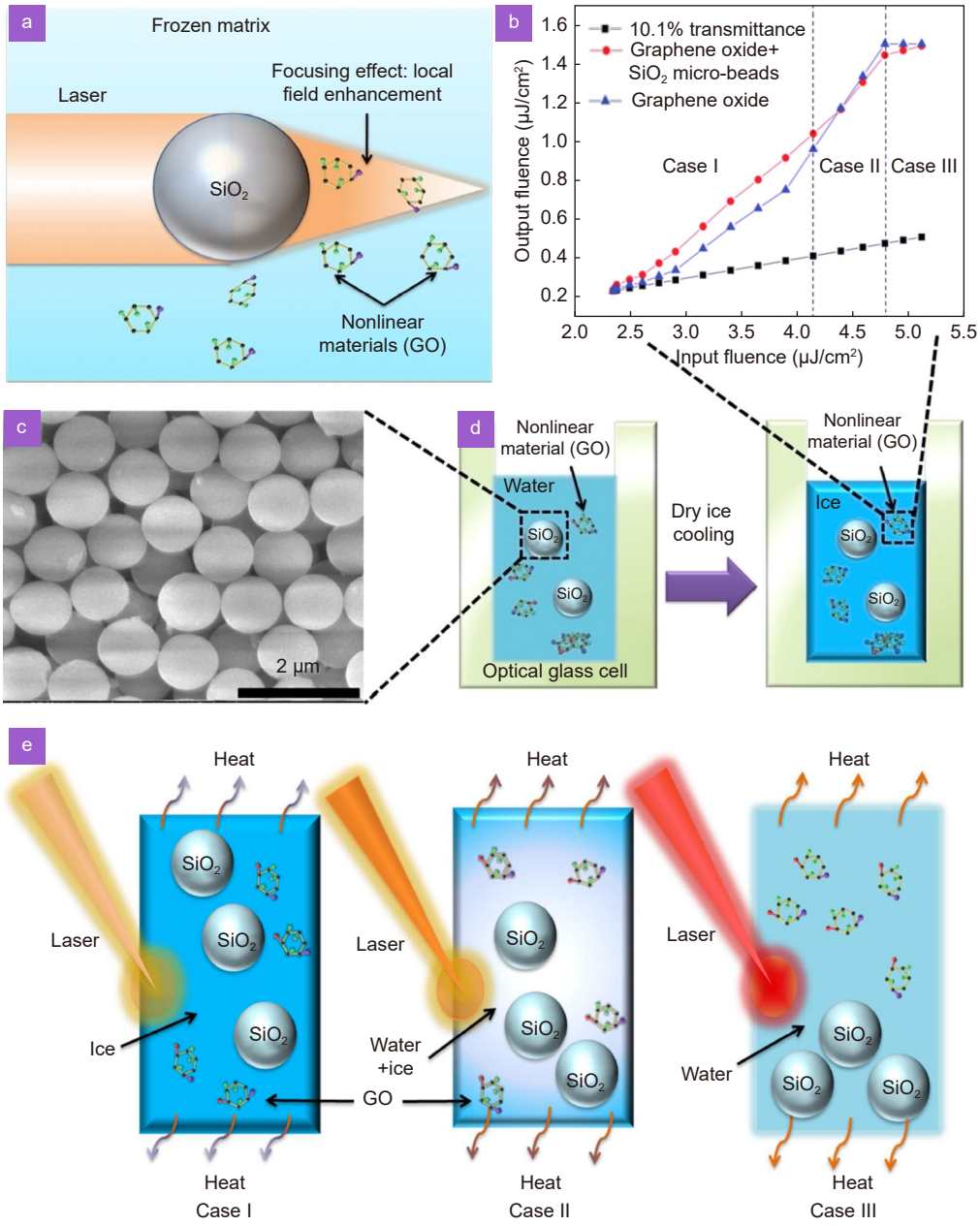

Fig. 7 | Dynamic nonlinear optical systems based on nanoparticles. (**a**) Schematic to demonstrate GO+microsphere system in the frozen matrix. Local field enhancement improves the optical nonlinearity of GO. (**b**) Nonlinear optical characterization to demonstrate the saturable absorption performance. (**c**) SEM image of microspheres mixed inside the frozen matrix. (**d**) Steps to show the preparation process to mix the GO and microspheres in the frozen matrix. (**e**) Nonlinear optical performance of the phase change system under incident light at different intensities. Figure reproduced with permission from ref.[125], The Royal Society of Chemistry.

sample. Samples with GO demonstrate nonlinear behaviors from 2.5 to 5.5 μJ/cm². At the low incident fluence below 4.2 μJ/cm², the transmittance keeps increasing, which is the feature of the saturable absorption In this process, samples with silica microspheres show enhanced nonlinearity. When the incident laser fluence exceeds 4.2 μJ/cm², the transmittance of the pure GO sample turns out to be similar to the GO + microsphere mixture. This process is illuminated by Fig. 7(e). The energy required to melt the frozen matrix is calculated. It is found that the incident laser fluence is sufficient to raise the temperature of the frozen matrix above its melting point. However, in the characterization process, the sample is maintained in an environment with frozen CO_2 (dry ice). The matrix stays frozen when the incident laser fluence is low. When the laser energy absorbed exceeds the cooling capacity, the matrix starts to melt and behave differently. When the frozen matrix partially

melts, the transmission of the system starts to increase due to the reduced scattering. As the microspheres have a higher density than water, they also start to precipitate and the nonlinearity enhancement effect is reduced. The transmittance reaches the maximum point at the laser fluence of 4.7 μJ/cm^2. At this laser fluence, the frozen matrix fully melts. When the laser irradiation is stopped, the liquid freezes quickly in a cool environment. In this process, laser energy is absorbed by the frozen matrix to protect the system from possible optical damage. Such a scheme is also widely compatible with various nonlinear materials. The frozen matrix can also prevent the aggregation of dispersed particles.

Despite the advantages of the frozen matrix, it requires the entire system to be in a cooled environment. The further development replaces water with a solid-state organic matrix as demonstrated in Fig. 8. To prepare this system, pulsed laser ablation is firstly applied to synthesize the silicon nanoparticles in water. The nanoparticles have a size distribution ranging from 200 nm to 800 nm. Most of them have the spherical shape. Gel wax is chosen as the phase change matrix. It is an organic material made up of mineral oils and polystyrene, which is transparent for visible and near IR wavelengths. To mix the silicon nanoparticles' with the gel wax, gel wax is firstly melted in a beaker on a hotplate. The silicon nanoparticle dispersion is added into the gel wax and heated up to the temperature of 95 °C. At this temperature, the

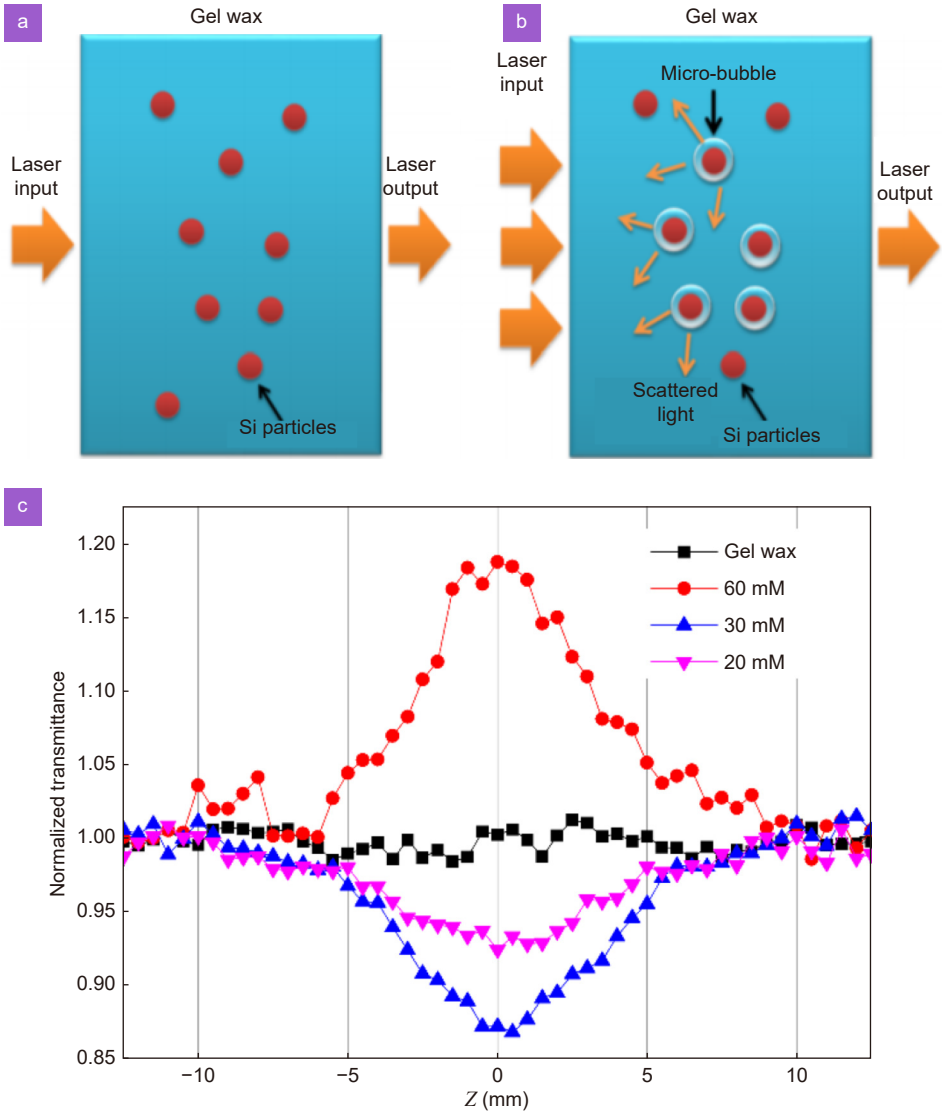

Fig. 8 | Nonlinear optical systems based on solid-state phase change material. (**a**) Nonlinear optical performance of phase change system under low laser fluence. Saturable absorption of silicon nanoparticles plays a dominant role. (**b**) Performance of phase change system under high laser fluence. Nonlinear scattering induced by the formation of the micro-bubbles plays a dominant role. (**c**) Z-scan characterizations on the tunable nonlinear optical performance of the phase change system. Figure reproduced with permission from ref.[72], Optical Society of America.

gel wax stays in the liquid phase. The mixture is stirred until all water is evaporated. In this process, silicon nanoparticles are transferred into the gel wax. The final product is collected and ultra-sonicated for 1 minute to ensure the silicon nanoparticles are well dispersed inside the matrix. The mixture is then put in room temperature to cool down until it is fully solidified. The positions of the nanoparticles in the gel wax are fixed. To measure the optical nonlinearity, Z-scan measurement is conducted at different laser fluences. The laser wavelength, pulse duration, and repetition rate are 800 nm, 100 fs, and 1 kHz, respectively. The thickness of the sample is 1 mm. The results of the Z-scan are demonstrated in Fig. 8(b). The black line in the plot indicates that the gel wax does not show any optical nonlinearity. The nonlinearity of the system is dominated by the concentrations of the silicon nanoparticles. When the concentration of Si nanoparticles increases from 20 mM to 30 mM, the peak transmittance decreases from 0.924 to 0.868. It demonstrates typical features of optical limiting. This nonlinear behavior is due to the nonlinear scattering of the laser irradiation on the nanoparticles' surfaces, as indicated in Fig. 8. Within this concentration range, additional nanoparticles impose more nonlinear scattering of incident light and the optical limiting effect is enhanced when the concentration increases. When the concentration is further increased to 60 mM, the nonlinear performance changes from optical limiting to saturable absorption. The physics behind can be explained as follow: at a concentration higher than a threshold, the smaller interparticle spacing of nanoparticles gives a higher possibility for the scattered laser light to interact strongly with neighboring nanoparticles. Hence, the saturable absorption of the nanoparticles dominates the nonlinear effect. Such switching of the nonlinear responses makes this system useful to construct many novel nonlinear devices. Gel wax is chemically stable and melts easily. Similar to the frozen matrix, the melting of the gel wax can protect the nanoparticles from optical damage, which increases the damage threshold and improves the stability of the nonlinear system.

Applications for nonlinear optical nanoparticles

Nonlinear optics offers effective methods for wavelength engineering, frequency doubling, wave mixing, and multiphoton absorption[104]. It is also the foundation for many other optical modulations, such as optical limiting, pulse modulation, and phase conjugation. Many widely used conventional optical devices rely on nonlinear performances, including laser sources, optical communication devices, and various types of sensors[105,106]. New nonlinear materials are also explored for state-of-art devices and systems. They are widely used in most frontier researches, such as the quantum technology, topological devices, and information processing. There are many types of nonlinear optical effects and these applications cannot be fully covered in the limited scope of this review. In this section, we will focus on the applications related to the third order nonlinearity, more specifically, the optical limiting and saturable absorption. Due to nanoparticles' small size, it is challenging for a single nanoparticle to form a device. Instead, a functional system is normally made of a large number of nanoparticles. Nanoparticles are the building blocks to make optical nonlinear materials of various types. For example, they can be mixed inside the solid matrices, dispersed inside the liquid matrix, and deposited into thin films. For specific bio-medical applications, nonlinear nanoparticles are directly injected into the animal body or fed into cells[107]. Various techniques are also invented to pattern, engineer, and further process optical nonlinear materials in order to fabricate new functional devices[31,108].

Optical limiting is one important nonlinear behavior based on the third-order nonlinearity. The applications for optical limiting can be widely found in systems with high energy. Optical limiting material is commonly used as a protective component against strong laser power that may cause damages. Among high energy systems, devices with high power laser sources are good examples to illuminate the functions of optical limiters. High power lasers have wide applications and protective devices are critical. For example, glass made of optical limiting materials is used in high power laser processing systems[109–111]. In these devices, optical limiter not only protects persons to operate the system. They can absorb the excess laser power above the threshold and protect the device from optical damage. Without optical limiters, the lifetime of these systems is greatly limited. Optical limiters based on nonlinear optical nanoparticles offer several advantages. They can be made into different shapes including thin films, glass doped with nonlinear particles, or even disperse into the liquid. This flexibility can fit different requirements and install flexibly in the high power laser systems. Furthermore, as a protective component, the optical limiter itself is easily damaged. Systems based on specific nanoparticles offer self-repairing

capabilities as discussed in the previous section. For the liquid-based nonlinear systems, additional nanoparticles can be flexibly added into the liquid to maintain its functionality. Another important application is protective components for optical sensors, which links to broad research areas and industries. Almost all optical sensors need to be protected against high power input signals to prevent saturation or damage. Due to these advantages, optical limiters based on nanoparticles are promising for many emerging new devices, such as high power laser weapons. Huge potential is yet to be discovered.

Beyond high energy applications, optical limiting materials can also be used for the low energy components. For example, optical limiting materials are used to construct the sensors for laser-guided weapons. In the laser-guided weapons, the seeker is one component to guide the weapon towards the target, which is critical for the accurate tracking[112]. Anti-jamming is a critical function for these seekers. Anti-jamming involves the process to filter out the noises, which prevents the enemy's interference. Many anti-jamming components are used, such as the narrowband filter in the front of the seeker and the tracking gate processing circuit in the signal processing part. However, these anti-jamming components are designed for low power jamming noises, which can be easily saturated if the incident light signal is too strong. For the practical cases, many environmental signals and noises with high intensities can interfere with the function of the seeker and disable it. Optical limiter is critical to filter out these high power noises. Specifically, these optical limiters need to react fast and offer a wide absorption spectrum, which matches the advantages of the nanoparticle based nonlinear systems. Multiple types of nanoparticles can be mixed together to provide protection across a broad range of wavelengths. With this protective component, the laser seeker can overcome its limitation and become capable to tackle the high power noises in a complicated environment[112]. This application demonstrates that optical limiter is effective to function as filters. It can be helpful for many sensing and imaging systems which are used to capture weak signals.

Besides the optical limiting, nanoparticles with saturable absorptions also have broad applications. Systems based on this nonlinearity are generally denoted as saturable absorbers. The most extensively used application of saturable absorbers is the functional material to achieve passive Q-switching or mode-locking for laser cavities. The roles of optical nonlinearities for Q-switching were fully explained by Nicolaas Bloembergen, who won the Nobel prize in 1981 for this work. It is achieved by putting the saturable absorber inside the laser cavity. The saturable absorber can be a piece of transparent solid doped with optical nonlinear nanoparticles. Initially, the laser medium is pumped and the saturable absorber has high absorption. When the light power stored in the cavity is low, the saturable absorber functions like a "Gate" to store and keep the energy within the cavity. As the amount of energy stored in the cavity increases, the rate of the stimulated emission for lasing also keeps increasing until it reaches the threshold of the saturable absorber. Above the threshold, the absorption of the saturable absorber decreases and the resonator loss reduces. Hence, the saturable absorber becomes more transparent and the "Gate" is open. The energy stored is released to produce a pulse with high peak energy. Then, the saturable absorber recovers to its initial state of high absorption, storing energy until the next pulse can be released. In this process, the properties of the saturable absorber directly affect the repetition rate and pulse duration. Furthermore, nanoparticles based saturable absorbers with a small footprint and enhanced function can also be used for solid-state and micro-chip lasers.

Saturable absorbers have been used for passive mode locking since the early 1970s. It was the only method available for this purpose until the invention of additive-pulse mode locking[113]. The basic mechanism behind the mode locking is easily understood by considering a fast saturable absorber whose absorption can change on a timescale of the pulse width. When an optical pulse propagates through such an absorber, the head and tail experience more loss than the central part, as the central part is intense enough to saturate the absorber. As a consequence, the light energy in the head and tail of the pulse are reduced and the pulse duration is shortened. The reduction of the pulse duration also leads to the generation of more intense pulses. This mechanism is widely used in the cavity of the fiber lasers and dye lasers. For these lasers, the saturable absorber with a fast response time is required, which can be achieved by mixing optical nonlinear nanoparticles inside a solid-state or liquid matrix. To construct the cavity, the saturable absorber can also be coated on one side of the cavity mirror. The saturable absorber can be made using either a single layer or a large stack (>100 layers) of layers. For multiple layers, it forms a periodic structure named a superlattice to further enhance the performance.

The saturable absorber can also be used as the nonlinear element for optical regeneration. Optical regenerators are critical for communication and information technologies. An optical generation needs to filter out the noise, distortion, and fluctuations in the optical signal. The operation principle of the saturable absorber is straightforward. When an optical signal with relatively low intensity transmits through the saturable absorber, the intensity is below the threshold of saturable absorption and the absorption is high. This makes the saturable absorber opaque to the signal. Noises are mostly of much lower intensities compared to the optical signal. In this case, these low-intensity components are filtered out by the saturable absorber. Different technologies to implement saturable absorbers are available. Semiconductor based nonlinear nanoparticles can provide excellent performance. Multiple layer structures with nanoparticles embedded can also be considered. The time to recover from a saturated state and the threshold is critical parameters. Doping can be used to further modify the properties of saturable absorbers.

Challenges and future technology development

An increasing number of research works are devoted to further enhancing the performance, extending functionalities, and optimizing parameters of nonlinear optical nanoparticle systems to fulfill customized demands for new applications. As conventional nanoparticles are approaching their limits, it becomes challenging for significant technology improvement or breakthrough, which is attributed to intrinsic limitations of materials properties. New functional nanoparticles offer new routes for continuous improvement to overcome these limitations. More opportunities keep emerging as various nonlinear optical nanoparticle systems are intensively investigated. For these nanoparticles' systems, breakthroughs are demanded to address two existing fundamental challenges: 1) **Morphology control**. Nanoparticles ranging from ~1 nm to ~10 μm can be synthesized by laser ablation. For many applications, monodisperse nanoparticles are demanded. As direct laser ablation can result in a large size distribution, accurate size control or selection in different environments is a critical issue. Furthermore, most nanoparticles demonstrate irregular or spherical shapes. How to produce nonlinear optical nanoparticles with arbitrary morphologies and shapes is another challenge. 2) **Productivity**. In laser ablation, the synthesis of nanoparticles only happens in the limited region of the laser focus spot. Hence, the productivity of nanoparticles by laser ablation was restricted. Other synthesis methods, such as chemical reactions, can easily achieve high productivity at kilogram-scale or even higher[114]. Control of the quality and yields are the other two issues, which need to be well considered for mass production[115]. Both issues are closely related to the dynamics of the high power pulsed laser ablation. While methods and recent progress to engineer the morphologies of nanoparticles are introduced in section nonlinear optical nanoparticles' production, functions, and applications, how to improve the productivity for laser ablation is important. A few new routes were reported to improve the functionalities and efficiency of the laser ablation. These methods can be classified into two groups. The first group involves the modification of the optical system: 1) **Hybrid laser irradiation:** Continuous-wave laser irradiation can be applied to enhance the nanosecond pulsed laser ablation. The continuous laser irradiation raises the surface temperature around the spot of laser ablation, which enhances the pulsed laser ablation at a much improved efficiency[116]. 2) **Double pulse spatial laser ablation:** Spatial double-pulsed laser ablation is another new approach to increase the laser ablation efficiency. Two splitted laser beams simultaneously irradiate on the silicon surface. It is reported that when the process parameters of the dual laser beams are properly tuned, the efficiency of such double-pulse laser ablation can be significantly enhanced by more than 65%[117]. 3) **Double pulse temporal laser ablation:** Further investigation is also conducted to study the effect of two overlapping laser pulses irradiating with a tunable time delay. It is found that the temporal control of two laser pulses can further influence the performance of the laser ablation. In the optimized condition, the laser ablation efficiency can achieve a 338% improvement compared to the single pulse laser ablation[118]. The second group of new approaches involves the modification of the matrix and substrates. The addition of surfactants is a common practice well-known for morphology modifications. Furthermore, other explorations demonstrate additional possibilities. Steam-assisted laser ablation of the solid substrate is investigated on multiple materials including Si, Cu, and mold components for the integrated circuit. A thin layer of steam is reported to significantly improve the laser ablation efficiency. The ablation rate is improved by 1.5 times[56,119].

Conclusions

The nanoparticle is an important candidate for nonlinear optical materials. Laser ablation is proven to be a flexible, fast, and effective fabrication approach for nanoparticles' synthesis with many advantages. Laser ablation is convenient for researchers as one laser ablation system can fabricate a great number of different materials within a short time, which can fulfill the needs for various applications. In this review, the physics, experimental system, parameter selection for laser ablation, results of nonlinear optical nanoparticles, and applications are summarized, which introduces the opportunities in this research field. Beyond the topics covered, nonlinear optical components are essential for various emerging research frontiers, such as ultrafast optics, high power lasers, nano-photonics, and information processing for artificial intelligence. The search for the best optical nonlinear materials for these fast- developing directions has attracted a lot of interests. Due to its straightforward process, fast speed, and flexible choice of materials, laser ablation can be a powerful technique to quickly find out the best nanoparticle to address these needs. It has been proven successful for many conventional applications and different types of laser synthesized nanoparticles have already been commercialized. For the emerging technologies, more potential is yet to be discovered.

References

1. Boyd RW. *Nonlinear Optics* 3rd ed (Academic Press, Waltham, 2008).
2. Kaneko K, Sun HB, Duan XM, Kawata S. Two-photon photoreduction of metallic nanoparticle gratings in a polymer matrix. *Appl Phys Lett* **83**, 1426–1428 (2003).
3. Camacho-Morales R, Rocco D, Xu L, Gili VF, Dimitrov N et al. Infrared upconversion imaging in nonlinear metasurfaces. *Adv Photonics* **3**, 036002 (2021).
4. Nauman M, Yan JS, Rahmani M, De Ceglia D, De Angelis C et al. Nonlinear transition-metal-dichalcogenide metasurfaces. In *14th Pacific Rim Conference on Lasers and Electro-Optics Pacific Rim (CLEO PR 2020)* 1–2 (OPTIC, 2020); http://doi.org/10.1364/CLEOPR.2020.C2E_4.
5. Chen JH, Shen XQ, Tang SJ, Cao QT, Gong QH et al. Microcavity nonlinear optics with an organically functionalized surface. *Phys Rev Lett* **123**, 173902 (2019).
6. Zhang SL, Liu LW, Ren S, Li ZL, Zhao YH et al. Recent advances in nonlinear optics for bio-imaging applications. *Opto-Electron Adv* **3**, 200003 (2020).
7. Zhang J, Sun TT, Zhang C, Yang YW, Lin CG et al. Enhanced third-order optical nonlinearity and photon luminescence of Sn^{2+} in gold nanoparticles embedded chalcogenide glasses. *J Mater Sci* **55**, 15882–15893 (2020).
8. Yang YW, Sun TT, Lin CG, Dai SX, Zhang XH et al. Performance modification of third-order optical nonlinearity of chalcogenide glasses by nanocrystallization. *Ceram Int* **45**, 18767–18771 (2019).
9. Zhang XY, Chen FF, Lin RQ, Huang YC, Dai SX et al. Investigation of third-order optical nonlinearities of copper doped germanium-gallium-sulfur chalcogenide glasses. *J Non-Cryst Solids* **475**, 167–171 (2017).
10. Zhang YN, Wu JY, Qu Y, Yang YY, Jia LN et al. Graphene oxide for enhanced optical nonlinear performance in CMOS compatible integrated devices. *Proc SPIE* **11688**, 116880W (2021).
11. Jia LN, Cui DD, Wu JY, Feng HF, Yang YY et al. BiOBr nanoflakes with strong Kerr nonlinearity towards hybrid integrated photonic devices. *Proc SPIE* **11282**, 112820Q (2020).
12. Zhang YN, Wu JY, Yang YY, Qu Y, Jia LN et al. Enhanced kerr nonlinearity and nonlinear figure of merit in silicon nanowires integrated with 2D graphene oxide films. *ACS Appl Mater Interfaces* **12**, 33094–33103 (2020).
13. Daniel MC, Astruc D. Gold nanoparticles: assembly, supramolecular chemistry, quantum-size-related properties, and applications toward biology, catalysis, and nanotechnology. *Chem Rev* **104**, 293–346 (2004).
14. Zhou R, Zhang Z, Hong MH. The art of laser ablation in aeroengine: the crown jewel of modern industry. *J Appl Phys* **127**, 080902 (2020).
15. Khew SY, Tan CF, Yan HP, Yan SD, Thian ES et al. Nanosecond laser ablation for enhanced adhesion of CuO nanowires on copper substrate and its application for oil-water separation. *Appl Surf Sci* **465**, 995–1002 (2019).
16. Zhou R, Yin YC, Long D, Cui JQ, Yan HP et al. PVP-assisted laser ablation growth of Ag nanocubes anchored on reduced graphene oxide (rGO) for efficient photocatalytic CO_2 reduction. *Prog Nat Sci:Mater Int* **29**, 660–666 (2019).
17. Yan HP, Xiao X, Chen ZL, Chen YS, Zhou R et al. Realization of adhesion enhancement of CuO nanowires growth on copper substrate by laser texturing. *Opt Laser Technol* **119**, 105612 (2019).
18. Zhou R, Yin YC, Liu YJ, Cui JQ, Li XG et al. Surfactant mediated synthesis of structured metal nanoparticle by pulsed laser ablation for photocatalysis. *Proc SPIE* **10842**, 108420F (2019).
19. Du ZR, Palina N, Chen J, Hong MH, Hoex B. Rear-side contact opening by laser ablation for industrial screen-printed aluminium local back surface field silicon wafer solar cells. *Energy Procedia* **25**, 19–27 (2012).
20. Hong MH, Sugioka K, Wu DJ, Wong LL, Lu YF et al. Laser-induced-plasma-assisted ablation for glass microfabrication. *Proc SPIE* **4595**, 138–146 (2001).
21. Lam HM, Hong MH, Yuan S, Chong TC. Laser ablation of GaN/sapphire structure for LED. *Proc SPIE* **4830**, 114–118 (2003).
22. Hong MH, Xie Q, Lim BC, Sugioka K, Midorikawa K et al. Low resistivity glass metallization by laser induced plasma-assisted ablation. *Proc SPIE* **5662**, 532–537 (2004).
23. Chichkov BN, Momma C, Nolte S, Von Alvensleben F, Tünnermann A. Femtosecond, picosecond and nanosecond laser ablation of solids. *Appl Phys A* **63**, 109–115 (1996).
24. Gamaly EG, Rode AV, Luther-Davies B, Tikhonchuk VT. Ablation of solids by femtosecond lasers: ablation mechanism and ablation thresholds for metals and dielectrics. *Phys Plasmas* **9**, 949–957 (2002).
25. Amendola V, Amans D, Ishikawa Y, Koshizaki N, Scirè S et al.

Room-temperature laser synthesis in liquid of oxide, metal-oxide core-shells, and doped oxide nanoparticles. *Chem – A Eur J* **26**, 9206–9242 (2020).
26. Yang GW. Laser ablation in liquids: applications in the synthesis of nanocrystals. *Prog Mater Sci* **52**, 648–698 (2007).
27. Amendola V, Meneghetti M. Laser ablation synthesis in solution and size manipulation of noble metal nanoparticles. *Phys Chem Chem Phys* **11**, 3805–3821 (2009).
28. Sakamoto M, Fujistuka M, Majima T. Light as a construction tool of metal nanoparticles: synthesis and mechanism. *J Photochem Photobiol C:Photochem Rev* **10**, 33–56 (2009).
29. Rehbock C, Jakobi J, Gamrad L, Van Der Meer S, Tiedemann D et al. Current state of laser synthesis of metal and alloy nanoparticles as ligand-free reference materials for nano-toxicological assays. *Beilstein J Nanotechnol* **5**, 1523–1541 (2014).
30. Asahi T, Sugiyama T, Masuhara H. Laser fabrication and spectroscopy of organic nanoparticles. *Acc Chem Res* **41**, 1790–1798 (2008).
31. Zhang DS, Gökce B, Barcikowski S. Laser synthesis and processing of colloids: fundamentals and applications. *Chem Rev* **117**, 3990–4103 (2017).
32. González-Rubio G, Guerrero-Martínez A, Liz-Marzán LM. Reshaping, fragmentation, and assembly of gold nanoparticles assisted by pulse lasers. *Acc Chem Res* **49**, 678–686 (2016).
33. Kanitz A, Kalus MR, Gurevich EL, Ostendorf A, Barcikowski S et al. Review on experimental and theoretical investigations of the early stage, femtoseconds to microseconds processes during laser ablation in liquid-phase for the synthesis of colloidal nanoparticles. *Plasma Sources Sci Technol* **28**, 103001 (2019).
34. Boyd RW. The intensity-dependent refractive index. In *Nonlinear Optics* 207–252 (2008); http://doi.org/10.1016/B978-0-12-369470-6.00004-6.
35. Shegai T, Li ZP, Dadosh T, Zhang ZY, Xu HX et al. Managing light polarization via plasmon–molecule interactions within an asymmetric metal nanoparticle trimer. *Proc Natl Acad Sci USA* **105**, 16448–16453 (2008).
36. Sheik-bahae M, Said AA, Van Stryland EW. High-sensitivity, single-beam n_2 measurements. *Opt Lett* **14**, 955–957 (1989).
37. Sheik-Bahae M, Said AA, Wei TH, Hagan DJ, Van Stryland EW. Sensitive measurement of optical nonlinearities using a single beam. *IEEE J Quantum Electron* **26**, 760–769 (1990).
38. Zhang JM, Claverie J, Chaker M, Ma DL. Colloidal metal nanoparticles prepared by laser ablation and their applications. *ChemPhysChem* **18**, 986–1006 (2017).
39. Ahmed N, Darwish S, Alahmari AM. Laser ablation and laser-hybrid ablation processes: a review. *Mater Manuf Process* **31**, 1121–1142 (2016).
40. Amendola V, Meneghetti M. What controls the composition and the structure of nanomaterials generated by laser ablation in liquid solution? *Phys Chem Chem Phys* **15**, 3027–3046 (2013).
41. Torrisi L, Torrisi A. Laser ablation of boron nitride in vacuum and in water. *Radiat Eff Defects Solids* **174**, 76–91 (2019).
42. Chen LW, Hong MH. Laser Surface Structuring of Semiconductors and Functionalization. *Handbook of Laser Micro- and Nano-Engineering*. in (ed. Sugioka K,) 1–45 (Springer International Publishing, 2020); http://doi.org/10.1007/978-3-319-69537-2_20-1.
43. Malinauskas M, Žukauskas A, Hasegawa S, Hayasaki Y, Mizeikis V et al. Ultrafast laser processing of materials: from science to industry. *Light:Sci Appl* **5**, e16133 (2016).
44. Amendola V, Meneghetti M. Controlled size manipulation of free gold nanoparticles by laser irradiation and their facile bioconjugation. *J Mater Chem* **17**, 4705–4710 (2007).
45. Xu KC, Zhang CT, Zhou R, Ji R, Hong MH. Hybrid micro/nanostructure formation by angular laser texturing of Si surface for surface enhanced Raman scattering. *Opt Express* **24**, 10352–10358 (2016).
46. Norton DP. Pulsed laser deposition of complex materials: progress toward applications. In *Pulsed Laser Deposition of Thin Films: Applications - Led Growth of Functional Materials* 1–31 (2006); http://doi.org/10.1002/9780470052129.ch1.
47. Amendola V, Rizzi GA, Polizzi S, Meneghetti M. Synthesis of gold nanoparticles by laser ablation in toluene: quenching and recovery of the surface plasmon absorption. *J Phys Chem B* **109**, 23125–23128 (2005).
48. Xiao J, Liu P, Wang CX, Yang GW. External field-assisted laser ablation in liquid: an efficient strategy for nanocrystal synthesis and nanostructure assembly. *Prog Mater Sci* **87**, 140–220 (2017).
49. Kazemizadeh F, Malekfar R, Parvin P. Pulsed laser ablation synthesis of carbon nanoparticles in vacuum. *J Phys Chem Solids* **104**, 252–256 (2017).
50. Schinca DC, Scaffardi LB, Videla FA, Torchia GA, Moreno P et al. Silver –silver oxide core –shell nanoparticles by femtosecond laser ablation: core and shell sizing by extinction spectroscopy. *J Phys D:Appl Phys* **42**, 215102 (2009).
51. Tan DZ, Zhou SF, Qiu JR, Khusro N. Preparation of functional nanomaterials with femtosecond laser ablation in solution. *J Photochem Photobiol C:Photochem Rev* **17**, 50–68 (2013).
52. Menéndez-Manjón A, Barcikowski S. Hydrodynamic size distribution of gold nanoparticles controlled by repetition rate during pulsed laser ablation in water. *Appl Surf Sci* **257**, 4285–4290 (2011).
53. Santillán JMJ, Videla FA, Van Raap MBF, Schinca DC, Scaffardi LB. Analysis of the structure, configuration, and sizing of Cu and Cu oxide nanoparticles generated by fs laser ablation of solid target in liquids. *J Appl Phys* **113**, 134305 (2013).
54. Wang HQ, Jia LC, Li L, Li XY, Swiatkowska-Warkocka Z et al. Photomediated assembly of single crystalline silver spherical particles with enhanced electrochemical performance. *J Mater Chem A* **1**, 692–698 (2013).
55. Sajti CL, Sattari R, Chichkov B, Barcikowski S. Ablation efficiency of α-Al_2O_3 in liquid phase and ambient air by nanosecond laser irradiation. *Appl Phys A* **100**, 203–206 (2010).
56. Hong MH, Koh ML, Zhu S, Lu YF, Chong TC. Steam-assisted laser ablation and its signal diagnostics. *Appl Surf Sci* **197–198**, 911–914 (2002).
57. Boyer P, Meunier M. Modeling solvent influence on growth mechanism of nanoparticles (Au, Co) synthesized by surfactant free laser processes. *J Phys Chem C* **116**, 8014–8019 (2012).
58. Du ZR, Chen LW, Kao TS, Wu MX, Hong MH. Improved optical limiting performance of laser-ablation-generated metal nanoparticles due to silica-microsphere-induced local field enhancement. *BEILSTEIN J Nanotechnol* **6**, 1199–1204 (2015).
59. Sylvestre JP, Kabashin AV, Sacher E, Meunier M. Femtosecond laser ablation of gold in water: influence of the laser-produced plasma on the nanoparticle size distribution. *Appl*

Phys A **80**, 753–758 (2005).
60. Tsuji T, Kakita T, Tsuji M. Preparation of nano-size particles of silver with femtosecond laser ablation in water. *Appl Surf Sci* **206**, 314–320 (2003).
61. Kuzmin PG, Shafee GA, Viau G, Warot-Fonrose B, Barberoglou M et al. Porous nanoparticles of Al and Ti generated by laser ablation in liquids. *Appl Surf Sci* **258**, 9283–9287 (2012).
62. Chen LW, Jiang XF, Guo ZM, Kao TS, Xu QH et al. Tuning optical nonlinearity of laser-ablation-synthesized silicon nanoparticles via doping concentration. *J Nanomater* **2014**, 652829 (2014).
63. Said A, Sajti L, Giorgio S, Marine W. Synthesis of nanohybrid materials by femtosecond laser ablation in liquid medium. *J Phys Conf Ser* **59**, 055 (2007).
64. Semaltianos NG, Logothetidis S, Perrie W, Romani S, Potter RJ et al. CdTe nanoparticles synthesized by laser ablation. *Appl Phys Lett* **95**, 033302 (2009).
65. Semaltianos NG, Logothetidis S, Perrie W, Romani S, Potter RJ et al. II–VI semiconductor nanoparticles synthesized by laser ablation. *Appl Phys A* **94**, 641 (2009).
66. Santagata A, De Bonis A, De Giacomo A, Dell'Aglio M, Laurita A et al. Carbon-based nanostructures obtained in water by ultrashort laser pulses. *J Phys Chem C* **115**, 5160–5164 (2011).
67. Teruki S, Tsuyoshi A, Hiroshi M. Formation of 10 nm-sized Oxo(phtalocyaninato)vanadium(IV) Particles by femtosecond laser ablation in water. *Chem Lett* **33**, 724–725 (2004).
68. Barcikowski S, Hahn A, Guggenheim M, Reimers K, Ostendorf A. Biocompatibility of nanoactuators: stem cell growth on laser-generated nickel –titanium shape memory alloy nanoparticles. *J Nanoparticle Res* **12**, 1733–1742 (2010).
69. Yamamoto T, Shimotsuma Y, Sakakura M, Nishi M, Miura K et al. Intermetallic magnetic nanoparticle precipitation by femtosecond laser fragmentation in liquid. *Langmuir* **27**, 8359–8364 (2011).
70. Stratakis E, Barberoglou M, Fotakis C, Viau G, Garcia C et al. Generation of Al nanoparticles via ablation of bulk Al in liquids with short laser pulses. *Opt Express* **17**, 12650–12659 (2009).
71. Podagatlapalli GK, Hamad S, Sreedhar S, Tewari SP, Rao SV. Fabrication and characterization of aluminum nanostructures and nanoparticles obtained using femtosecond ablation technique. *Chem Phys Lett* **530**, 93–97 (2012).
72. Zhou Y, Chen LW, Du ZR, Cao Y, Li FP et al. Tunable optical nonlinearity of silicon nanoparticles in solid state organic matrix. *Opt Mater Express* **5**, 1606–1612 (2015).
73. Chen GX, Hong MH, He Q, ChenWZ, Elim HI et al. Formation, structure and nonlinear optical properties of carbon nanoparticles synthesized by pulsed laser ablation. *Appl Phys A* **79**, 1079–1082 (2004).
74. Chen GX, Hong MX, Chong TC, Elim HI, Ma GH et al. Preparation of carbon nanoparticles with strong optical limiting properties by laser ablation in water. *J Appl Phys* **95**, 1455–1459 (2004).
75. Chen GX, Hong MH, Tan LS, Chong TC, Elim HI et al. Optical limiting phenomena of carbon nanoparticles prepared by laser ablation in liquids. *J Phys:Conf Ser* **59**, 289–292 (2007).
76. Josset S, Muller O, Schmidlin L, Pichot V, Spitzer D. Nonlinear optical properties of detonation nanodiamond in the near infrared: effects of concentration and size distribution. *Diam Relat Mater* **32**, 66–71 (2013).
77. Amans D, Diouf M, Lam J, Ledoux G, Dujardin C. Origin of the nano-carbon allotropes in pulsed laser ablation in liquids synthesis. *J Colloid Interface Sci* **489**, 114–125 (2017).
78. Yang GW, Wang JB, Liu QX. Preparation of nano-crystalline diamonds using pulsed laser induced reactive quenching. *J Phys:Condens Matter* **10**, 7923–7927 (1998).
79. Zhang CY, Wang CX, Yang YH, Yang GW. A nanoscaled thermodynamic approach in nucleation of CVD diamond on non-diamond surfaces. *J Phys Chem B* **108**, 2589–2593 (2004).
80. Kraus D, Ravasio A, Gauthier M, Gericke DO, Vorberger J et al. Nanosecond formation of diamond and lonsdaleite by shock compression of graphite. *Nat Commun* **7**, 10970 (2016).
81. Pearce SRJ, Henley SJ, Claeyssens F, May PW, Hallam KR et al. Production of nanocrystalline diamond by laser ablation at the solid/liquid interface. *Diam Relat Mater* **13**, 661–665 (2004).
82. Goh YW, Lu YF, Hong MH, Chong TC. Femtosecond laser ablation of copper. *Proc SPIE* **4830**, 442–446 (2003).
83. Tsuji T, Iryo K, Watanabe N, Tsuji M. Preparation of silver nanoparticles by laser ablation in solution: influence of laser wavelength on particle size. *Appl Surf Sci* **202**, 80–85 (2002).
84. Barcikowski S, Walter J, Hahn A, Koch J, Haloui H et al. Picosecond and femtosecond laser machining may cause health risks related to nanoparticle emission. *J Laser Micro/Nanoeng* **4**, 159–164 (2009).
85. Zijlstra P, Chon JWM, Gu M. White light scattering spectroscopy and electron microscopy of laser induced melting in single gold nanorods. *Phys Chem Chem Phys* **11**, 5915–5921 (2009).
86. Link S, Burda C, Mohamed MB, Nikoobakht B, El-Sayed MA. Laser photothermal melting and fragmentation of gold nanorods: energy and laser pulse-width dependence. *J Phys Chem A* **103**, 1165–1170 (1999).
87. Logunov SL, Ahmadi TS, El-Sayed MA, Khoury JT, Whetten RL. Electron dynamics of passivated gold nanocrystals probed by subpicosecond transient absorption spectroscopy. *J Phys Chem B* **101**, 3713–3719 (1997).
88. Cui H, Liu P, Yang GW. Noble metal nanoparticle patterning deposition using pulsed-laser deposition in liquid for surface-enhanced Raman scattering. *Appl Phys Lett* **89**, 153124 (2006).
89. Raveendran P, Fu J, Wallen SL. A simple and "green" method for the synthesis of Au, Ag, and Au–Ag alloy nanoparticles. *Green Chem* **8**, 34–38 (2006).
90. Lin XZ, Liu P, Yu JM, Yang GW. Synthesis of CuO nanocrystals and sequential assembly of nanostructures with shape-dependent optical absorption upon laser ablation in liquid. *J Phys Chem C* **113**, 17543–17547 (2009).
91. Boltaev GS, Ganeev RA, Krishnendu PS, Zhang K, Guo CL. Nonlinear optical characterization of copper oxide nanoellipsoids. *Sci Rep* **9**, 11414 (2019).
92. Liu CH, Hong MH, Zhou Y, Chen GX, Saw MM et al. Synthesis and characterization of Ag deposited TiO_2 particles by laser ablation in water. *Phys Scr* **2007**, 326–328 (2007).
93. Riabinina D, Durand C, Chaker M, Rowell N, Rosei F. A novel approach to the synthesis of photoluminescent germanium nanoparticles by reactive laser ablation. *Nanotechnology* **17**, 2152–2155 (2006).
94. Yoon HR, Jo W, Lee EH, Lee JH, Kim M et al. Generation of phase-change Ge–Sb–Te nanoparticles by pulsed laser ablation. *J Non-Cryst Solids* **351**, 3430–3434 (2005).

95. Zhu S, Hong MH, Koh ML, Lu YF. Laser ablation of Si in water and ambient air. *Proc SPIE* **4426**, 39–42 (2002).
96. He Y, Fan CH, Lee ST. Silicon nanostructures for bioapplications. *Nano Today* **5**, 282–295 (2010).
97. Sánchez CJE, Ramírez KME, Delgado SMA, De Guevara HPL, Contreras JC et al. Determination of non-linear optical properties of TiO_2 nanoparticles functionalized with an azo-triphenylmethane dye using the z-scan technique. In *Latin America Optics and Photonics Conference* Tu4A. 11 (Optical Society of America, 2018); http://doi.org/10.1364/LAOP.2018.Tu4A.11.
98. De Boni L, Barbano EC, De Assumpção TA, Misoguti L, Kassab LRP et al. Femtosecond third-order nonlinear spectra of lead-germanium oxide glasses containing silver nanoparticles. *Opt Express* **20**, 6844–6850 (2012).
99. Liu P, Wang CX, Chen XY, Yang GW. Controllable fabrication and cathodoluminescence performance of high-index facets GeO_2 micro- and nanocubes and spindles upon electrical-field-assisted laser ablation in liquid. *J Phys Chem C* **112**, 13450–13456 (2008).
100. Tian ZF, Liang CH, Liu J, Zhang HM, Zhang LD. Zinc stannate nanocubes and nanourchins with high photocatalytic activity for methyl orange and 2, 5-DCP degradation. *J Mater Chem* **22**, 17210–17214 (2012).
101. Wu J, Jia LN, Zhang YN, Qu Y, Jia BH et al. Graphene oxide for integrated photonics and flat optics. *Adv Mater* **33**, 2006415 (2021).
102. Loh KP, Bao QL, Eda G, Chhowalla M. Graphene oxide as a chemically tunable platform for optical applications. *Nat Chem* **2**, 1015–1024 (2010).
103. Zheng XR, Jia BH, Chen X, Gu M. In situ third-order non-linear responses during laser reduction of graphene oxide thin films towards on-chip non-linear photonic devices. *Adv Mater* **26**, 2699–2703 (2014).
104. Tan Y, Chen LW, Wang D, Chen YX, Akhmadaliev S et al. Tunable picosecond laser pulses via the contrast of two reverse saturable absorption phases in a waveguide platform. *Sci Rep* **6**, 26176 (2016).
105. Huang HZ, Li JH, Deng J, Ge Y, Liu HG et al. Passively Q-switched Tm/Ho composite laser. *Opto-Electron Adv* **3**, 190031 (2020).
106. Zhang XJ, Li WW, Li J, Xu HY, Cai ZP et al. Mid-infrared all-fiber gain-switched pulsed laser at 3 μm. *Opto-Electron Adv* **3**, 190032 (2020).
107. Wang F, Han Y, Lim CS, Lu YH, Wang J et al. Simultaneous phase and size control of upconversion nanocrystals through lanthanide doping. *Nature* **463**, 1061–1065 (2010).
108. Wang SH, Li YH, Little BE, Wang LR, Wang X et al. Athermal third harmonic generation in micro-ring resonators. *Opto-Electron Adv* **3**, 200028 (2020).
109. Hou YH, Liu B, Liu Y, Zhou YH, Song TT, Zhou Q et al. Ultra-low cost Ti powder for selective laser melting additive manufacturing and superior mechanical properties associated. *Opto-Electron Adv* **2**, 180028 (2019).
110. Liu XQ, Bai BF, Chen QD, Sun HB. Etching-assisted femtosecond laser modification of hard materials. *Opto-Electron Adv* **2**, 190021 (2019).
111. Xie XZ, Zhou CX, Wei X, Hu W, Ren QL. Laser machining of transparent brittle materials: from machining strategies to applications. *Opto-Electron Adv* **2**, 180017 (2019).
112. Niu YX, Wu DS, Zhang P, Duan XF. Application of optical limiting materials in laser seeker. *Proc SPIE* **5646**, 297–302 (2005).
113. Ma WZ, Zhao DS, Liu RM, Wang TS, Yuan Q et al. Observation and optimization of 2 μm mode-locked pulses in all-fiber net anomalous dispersion laser cavity. *Opto-Electron Adv* **3**, 200001 (2020).
114. Streubel R, Barcikowski S, Gökce B. Continuous multigram nanoparticle synthesis by high-power, high-repetition-rate ultrafast laser ablation in liquids. *Opt Lett* **41**, 1486–1489 (2016).
115. Chen LW, Yin YM, Li Y, Hong MH. Multifunctional inverse sensing by spatial distribution characterization of scattering photons. *Opto-Electron Adv* **2**, 190019 (2019).
116. Ding Y, Yang LJ, Hong MH. Enhancement of pulsed laser ablation assisted with continuous wave laser irradiation. *Sci China Phys, Mech Astron* **62**, 34211 (2019).
117. Zhou R, Lin SD, Ding Y, Yang H, Ong YKK et al. Enhancement of laser ablation via interacting spatial double-pulse effect. *Opto-Electron Adv* **1**, 180014 (2018).
118. Lin ZY, Ji LF, Hong MH. Enhancement of femtosecond laser-induced surface ablation via temporal overlapping double-pulse irradiation. *Photonics Res* **8**, 271–278 (2020).
119. Hong MH, Ng KY, Xie Q, Shi LP, Chong TC. Pulsed laser ablation in a cooled liquid environment. *Appl Phys A* **93**, 153–157 (2008).
120. Yang GW, Wang JB. Pulsed-laser-induced transformation path of graphite to diamond via an intermediate rhombohedral graphite. *Appl Phys A* **72**, 475–479 (2001).
121. Singh A, Kutscher HL, Bulmahn JC, Mahajan SD, He GS et al. Laser ablation for pharmaceutical nanoformulations: multi-drug nanoencapsulation and theranostics for HIV. *Nanomedicine Nanotechnol, Biol Med* **25**, 102172 (2020).
122. Chen GX, Hong MH, Lan B, Wang ZB, Lu YF et al. A convenient way to prepare magnetic colloids by direct Nd: YAG laser ablation. *Appl Surf Sci* **228**, 169–175 (2004).
123. Ong TS, Lee SS, Van LH, Hong MH, Chong TC. Optical limiting properties of silver nanoparticles fabricated by laser ablation. *Proc SPIE* **5662**, 67–70 (2004).
124. Jin YJ, Chen LW, Wu MX, Lu XZ, Zhou R et al. Enhanced saturable absorption of the graphene oxide film via photonic nanojets. *Opt Mater Express* **6**, 1114–1121 (2016).
125. Chen LW, Zheng XR, Du ZR, Jia BH, Gu M et al. A frozen matrix hybrid optical nonlinear system enhanced by a particle lens. *Nanoscale* **7**, 14982–14988 (2015).

Acknowledgements

The authors are grateful for the discussions with Dr. R. Zhou, Dr. G. X. Chen, Dr. H.G. Liu, Dr. Y. Z. Zhao, and Dr. Y. Zhou. This work was supported by Advanced Remanufacturing and Technology Centre (ARTC) under its RIE2020 Advanced Manufacturing and Engineering (AME) IAF PP Grant (No. A19C2a0019) and Ministry of Education — Singapore (MOE2019-T2-2-147).

Competing interests

The authors declare no competing financial interests.